Characterization of surface, subsurface and their effect on fatigue life after machining on Aerospace Grade Aluminum Alloy (Al 6082-T6)

Mr. Muhammad Jahanzeb Zia
NUST201363023MSMME62213F

Supervisor
Dr. Syed Hussain Imran Jaffery

Co-Supervisor
Dr. Mushtaq Khan

School of Mechanical and Manufacturing Engineering (SMME)
National University of Science and Technology (NUST),
H-12, Islamabad, Pakistan

June, 2017

Characterization of surface, subsurface and their effect on fatigue life after machining on Aerospace Grade Aluminum Alloy (Al 6082-T6)

Author

Muhammad Jahanzeb Zia

Regn Number

NUST201363023MSMME62213F

A thesis submitted in partial fulfillment of the requirements for the degree of

MS Mechanical Engineering

Thesis Supervisor:

Dr. Syed Hussain Imran Jaffery

Thesis Supervisor's Signature: _____

SCHOOL OF MECHANICAL & MANUFACTURING ENGINEERING

NATIONAL UNIVERSITY OF SCIENCES AND TECHNOLOGY,

ISLAMABAD

JUNE, 2017

Declaration

I certify that this research work titled "*Characterization of surface, subsurface and their effect on fatigue life after machining on Aerospace Grade Aluminum Alloy (Al 6082-T6)"* is my own work. The work has not been presented elsewhere for assessment. The material that has been used from other sources it has been properly acknowledged / referred.

Signature of Student

Muhammad Jahanzeb Zia

NUST201363023MSMME62213F

Plagiarism Certificate (Turnitin Report)

This thesis has been checked for Plagiarism. Turnitin report endorsed by Supervisor is attached.

Signature of Student

Muhammad Jahanzeb Zia

NUST201363023MSMME62213F

Signature of Supervisor

Copyright Statement

- Copyright in text of this thesis rests with the Muhammad Jahanzeb Zia. Copies (by any process) either in full, or of extracts, may be made only in accordance with instructions given by the author and lodged in the Library of NUST School of Mechanical & Manufacturing Engineering (SMME). Details may be obtained by the Librarian. This page must form part of any such copies made. Further copies (by any process) may not be made without the permission (in writing) of the author.
- The ownership of any intellectual property rights which may be described in this thesis is vested in NUST School of Mechanical & Manufacturing Engineering, subject to any prior agreement to the contrary, and may not be made available for use by third parties without the written permission of the SMME, which will prescribe the terms and conditions of any such agreement.
- Further information on the conditions under which disclosures and exploitation may take place is available from the Library of NUST School of Mechanical & Manufacturing Engineering, Islamabad.

Acknowledgements

I am thankful to my Almighty Allah to have guided me throughout this work at every step and for every new thought which You setup in my mind to improve it.

I am profusely thankful to my beloved parents who raised me when I was not capable of walking and continued to support me throughout in every department of my life.

I would also like to express special thanks to my supervisor Dr. Syed Hussain Imran Jaffery and co-supervisor Dr. Mushtaq Khan for their help throughout my thesis. I can safely say that I haven't learned any other engineering subject in such depth than the ones which he has taught.

I would also like to pay special thanks to Mr. Akseer and Mr. Waseem for their tremendous support and cooperation. Each time I got stuck in something, he came up with the solution. I appreciate their patience and guidance throughout the whole thesis.

I would also like to thank Dr. Liaqat Ali and Dr. Aamir Mubashir for being on my thesis guidance and evaluation committee.

Finally, I would like to express my gratitude to all the individuals who have rendered valuable assistance to my study.

Dedicated to my exceptional parents and adored siblings whose tremendous support and cooperation led me to this wonderful success.

ABSTRACT

Aluminum alloys are widely used in automotive and aerospace industry due to their lower mass to strength ratio than other metallic alloys. Apart from their inherent properties, aluminum alloys like other metallic alloys shows significant change in their mechanical properties like fatigue, hardness etc. according to the machining parameters like speed of cut, nose radius of tool, coolant, feed rate, etc. that relates to the change in grain structure. Knowledge of optimized parametric selection is very important in machining of aluminum alloys in context of their mechanical behavior. In this research, the effect of different machining parameters on the subsurface of aerospace grade aluminum alloy (Al-6082-T6) was observed. Feed rate, cutting speed and depth of cut were the key machining parameters that were considered. The main result focused was the depth of subsurface damage caused by these machining parameters. ISO 3685 was followed for selecting cutting parameters and their range was selected by tool manufacturer's catalogue i.e. Sandvik Coromant Catalogue 2011 and Corokey of the Sandvik Coromant Catalogue 2011. All of 27 samples, according to Design Expert software, were prepared on CNC machine with 3 of variable values of cutting speed, feed rate and depth of cut. These samples were prepared for metallography by mounting, grinding, polishing and etching. ISO 4287:1997 is followed for surface roughness parametrical study. According to ASTM E384 and E92 micro hardness tests were carried out down the edge of the cross section of sample. Results of surface roughness and micro hardness tests are compared with fatigue life. Results are discussed along with recommendations for optimized machining parameter to achieve desirable mechanical properties of material (surface roughness, subsurface hardness and fatigue life).

Key Words: Surface roughness, subsurface damage, turning of aluminum, subsurface hardening

Table of Contents

Table of Figures

Table of Tables

Chapter 1: Introduction

1.1 Introduction

Machining of material is a key process that control mechanical parameters along with the type of material. Type of machining to be carried is directly associated with the fatigue life of the manufactured part. Fatigue is due to plastic deformation due to cyclic loading. Localized crack propagate due to plastic deformation usually from the upper layers of the part. Surface and subsurface parameters are of key importance in the propagation of these cracks. Machining parameters and their optimization is of extreme valued in this regard.

Aluminum Al-6082 is widely used in aerospace, automobiles and naval transport industry due to its high strength to weight ratio. In context of its high usage in the industry where cyclic loading is very common the study of its fatigue life is extremely important. Due to its good machinability aluminum is favorite for every manufacturing industry. As its machinability is concerned its effect on fatigue is considerable. In fatigue, crack develops from surface and higher subsurface level so effect of machining on these two parameters and optimized machining parameters` selection is very important to observe and control this mechanical property.

In this research, surface roughness and subsurface damage due to machining at different parameters are compared with fatigue life of the aluminum. Optimized parameters are also discussed. Machining parameters that are considered includes cutting speed, feed rate and depth of cut. Response of these machining factors is separately studied on surface roughness, subsurface damage and their effect on fatigue life.

Aluminum Al-6082-T6 material is used for sample preparation according to fatigue life sample preparation standards. For rotating fatigue life testing, ISO 1143:2010 standard is used that guide about the dimensions of specimen, machining procedure, handling, accuracy of test, test procedure and representation of fatigue life test results. Loading on specimen is at four points.[1]

Machining parameters are selected from the manufacturer`s catalogue ‘Sandvik Coromant Catalogue 2011 and Corokey of the Sandvik Coromant Catalogue 2011` and finalized by ISO 3685 standard for tool life testing with single point turning tool. [1]

Design of experiment is selected on the basis of all possible combination of these parameters (exhaustive testing). These combinations includes three values of feed rate, cutting speed and depth of cut each.

Turning is carried on Al-6082-T6 pieces according to the standard and fatigue life results are obtained. Separate samples are turned according to the DOE to investigate the effects of surface roughness and subsurface damage by micro hardness method.

Surface roughness of turned surfaces are carried according to the standard ISO 4287:1997. Each result is validated with repetition of three times.

Micro hardness test is carried out radially in the depth of cross sectional part of the machined specimen. These tests are carried out according to the standard ASTM E384 and E92 that guide about the specimen preparation, measurement of indents, indent distances and reading of the results. For sample preparation of subsurface hardness checking, specimens that turned according to the DOE is cross-sectionaly sectioned. For surface finish and microscopy, these samples are mounted, grinded and polished to a fine scratch less surface by carrying each process into different stages. Six indents in a row is carried to observe the damage depth with respect to the hardness of material with the repeatability of three times on each sample perpendicular to the machined surface along the radial side. Temperature gradient effects the microstructure of the material that results in change in mechanical properties.[2]

In addition to that, micro hardness is compared for hot mounting and cold mounting and compared their results to study the effect their effects on material hardness. Scanning electron microcopy and microstructure results for different etchants and methods carried out for sample preperation.

Results are discussed with the help of graphs and plots of surface roughness and micro hardness tests due to the effect of feed rate, cutting speed and depth of cut separately and also the effect of surface roughness and micro hardness compared to the fatigue life of the specified samples. Optimized parameters for surface roughness, micro hardness and fatigue life effects are also discussed.

1.2 Aims

Aim is to study the effect of machining parameters on surface roughness and subsurface hardness and their effect on the fatigue life of aerospace grade aluminum (Al-6082-T6)

1.3 Objectives

Objective of this research is to:

1. Carry out literature review on machining effect on aluminum alloys.
2. Carry out literature review for microstructure changes of metallic machining.
3. Carry out literature review on the effect of machining on surface roughness of aluminum alloys.
4. Carry out literature review on the effect of machining on subsurface hardness of metals.
5. Carry out literature review on micro hardness testing and sample preparation for microscopy.
6. Carry out literature review on effect of surface roughness and subsurface damage on fatigue life of metals.
7. Carry out design of experiment and selection of factors and responses for the experiment.
8. Sample preparation of aluminum by different processes like turning, sectioning, mounting, grinding, polishing and etching.
9. Perform surface roughness experiment.
10. Perform micro hardness experiment.
11. To study the effect of hot and cold mounting on micro hardness.
12. Analyze the tests data results.

Chapter 2: Literature Review

2.1 Mechanical Behavior of Al-6082-T6 alloy welds

S. Messori et al., investigated the rotating fatigue life and micro hardness at the welded region and compared with the grain structure analyzed with the SEM. Six samples were prepared depending on different parameters of Gas metallic Arc Welding (GMAW). That were proceeded to mechanical tests like tensile test, vicker micro hardness test, fatigue rotating test and charpy V-test.[3]

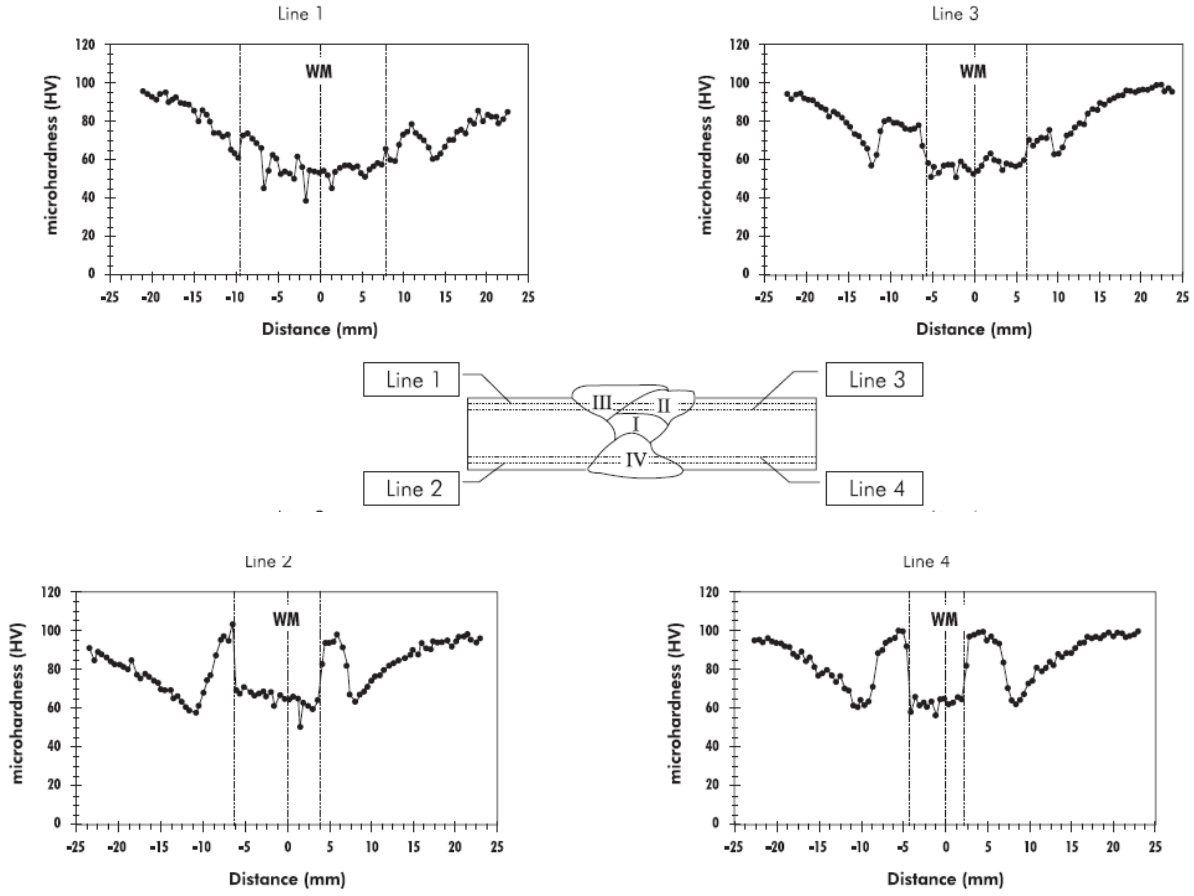

Fig. 1 Vickers hardness test survey on welded region

Vickers micro hardness test shows the hardness decreases in WM to 60Hv average while in heat affected zone (HAZ) it is 80 Hv and in base material its value is 100Hv. Fatigue test performed that shows most of the samples failed from HAZ region.

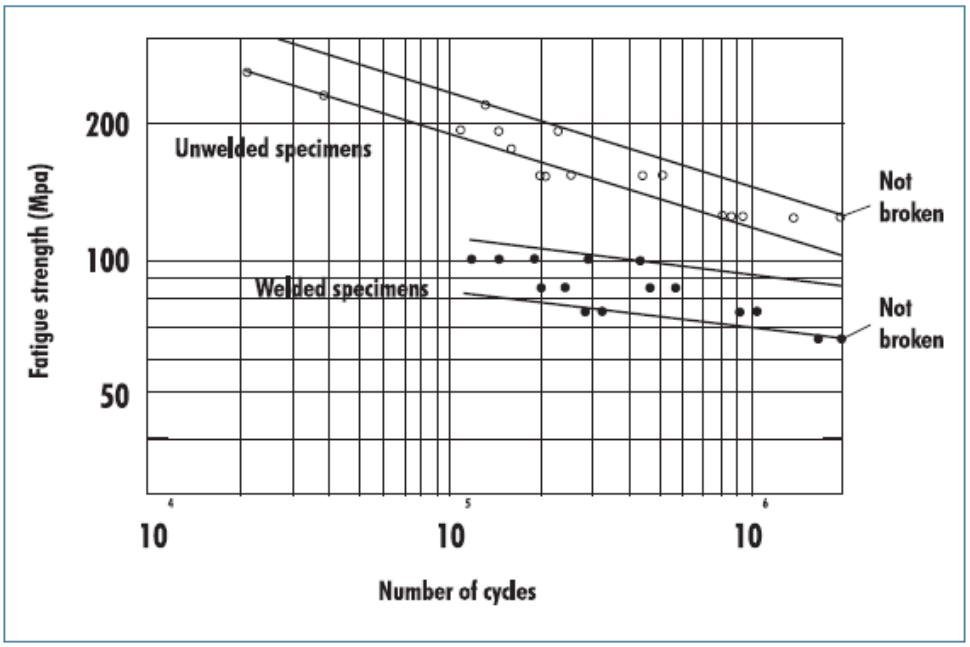

Fig. 2 Fatigue life test for welded and un welded samples.

Fatigue rupture stress for un welded samples are 130-280 MPa and for welded this value reduce to 70 to 100 MPa.

It was concluded that welded material fracture earlier than un welded material. In HAZ, both hardness and tensile strength reduce to its minimum value and SEM images shows that during fatigue life testing most samples fails in HAZ.[3]

Mufti et al., studied the effect of micro hardness on machining of deposition in Gas Metal Arc Welding (GMAW). Two samples were prepared i.e. deposition with intermediate machining (GWIM) and deposition without machining (GWM) and hardness test was conducted. [2]

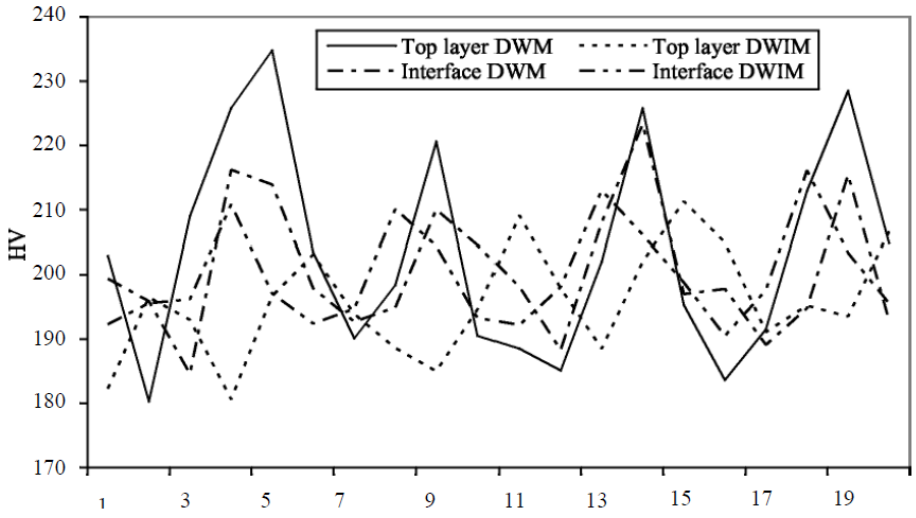

Fig. 3 Hardness of layers along deposition in mm

Average hardness is in GWM is higher that is 202.98Hv whereas for GWIM samples this value is 194.1Hv due to removal of top layer. While interface layer of GWIM had higher hardness than GWM samples.[2]

2.2 Surface roughness and subsurface damage relationship

Blaineau et al., studied the relation of surface roughness with subsurface damage of fused silica using Abbot Firestone curve. Nine samples were prepared at different parameters load, grinding speed, abrasive, abrasive size and slurry concentration. Surface roughness was measured by surface profile meter and subsurface damage by etching of samples.

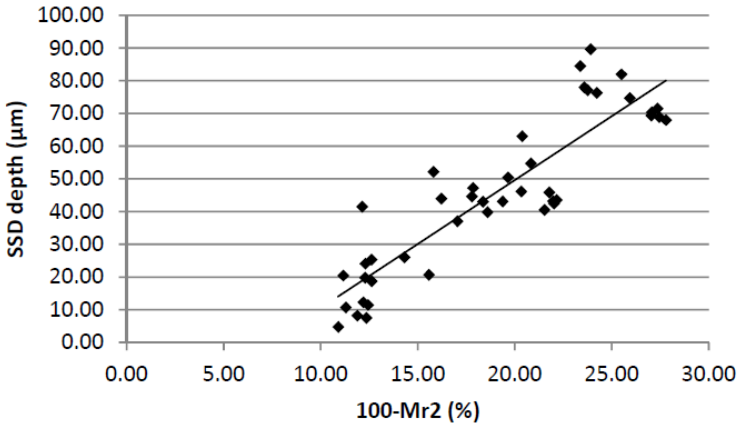

Fig 4, SSD and 100-Mr2 (%) of whole set

It was concluded that fraction of valley roughness profile (100-Mr2), calculated by Abbot-Firestone curve, is in linear relationship SSD and is more accurate indicator than maximum peak to valley roughness (Rtmax).[4]

Dobrescu et al., studied the comparative study of subsurface damage and surface roughness of silicon ceramics. Samples were prepared under different conditions and observed under Scanning Electron Microscopy for subsurface damage and profile meter for surface damage. Different grit grinders are used under different load conditions for silicon nitride and silicon carbide.

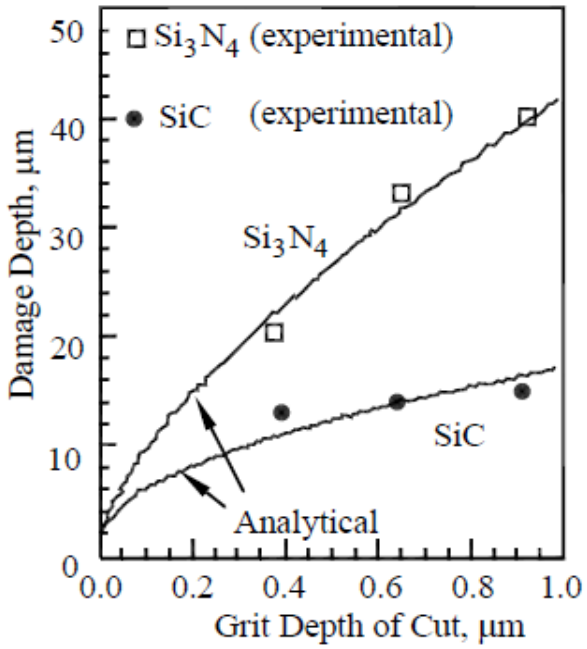

Fig. 5 Damage depth vs Grit depth of cut

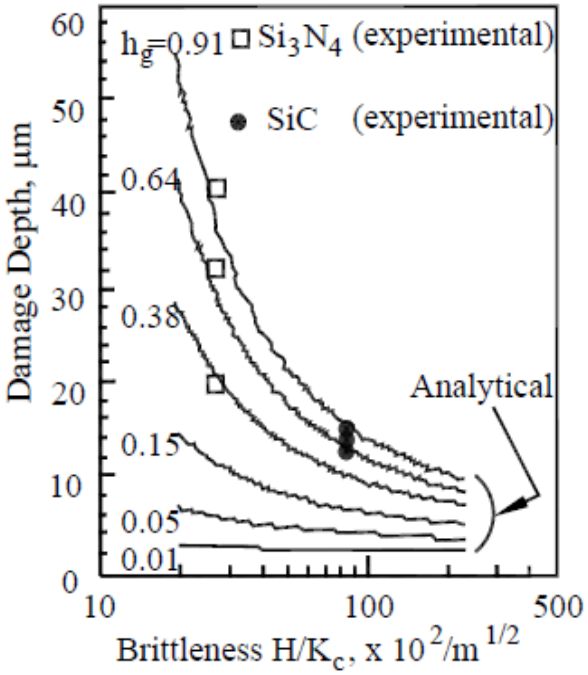

Fig. 6 Damage Depth vs Brittleness

Results showed that penetration depth of subsurface damage depends on ceramic type, Brittleness and maximum grit of depth of cut.[5]

2.3 Machining effect on mechanical parameters on titanium nickel alloys

Durul Uultan et al. studied the effects on machining on mechanical properties of Ti-Ni alloys especially subsurface and microstructure disturbances. During machining processes, material is exposed to thermal, mechanical and chemical energy. Due to strain aging process material becomes harder and more brittle. Micro structure of material changes underneath the surface of machining usually due to cutting speed and feed rate in turning. A white layer is formed that is much harder than the base material. White layer is also most commonly supportive to the crack propagation.[6]

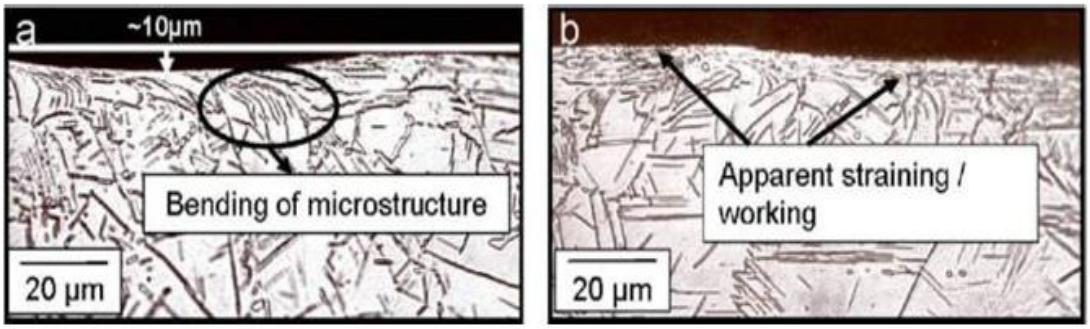

Fig. 7. Microstructural alterations in feed direction after end milling IN-718 at V=90 m/min, f=0.2 mm/tooth, and DoC=0.5 mm [44].

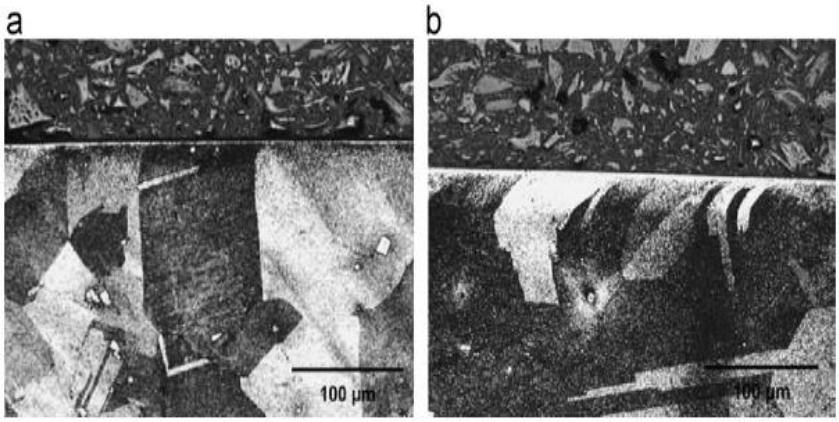

Fig. 8. Microstructural deformations of turned IN-718 at V=40–120 m/min, f=0.15–0.25 mm/rev, DoC=0.25 mm with (a) new tool and (b) worn tool [40].

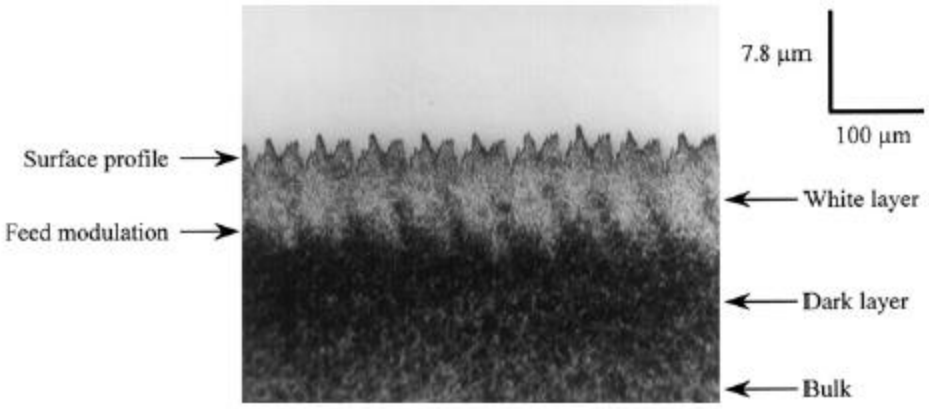

Fig. 9 Layers created after hard turning of steel

Another most common phenomenon is plastic deformation of material due to machining. Significant parameters of are machining are feed rate, depth of cut and cutting speed. A work hardening layer is formed due to the above mentioned parameters. Tool life is also specifically remarked factor in the formation of these layers. [6]

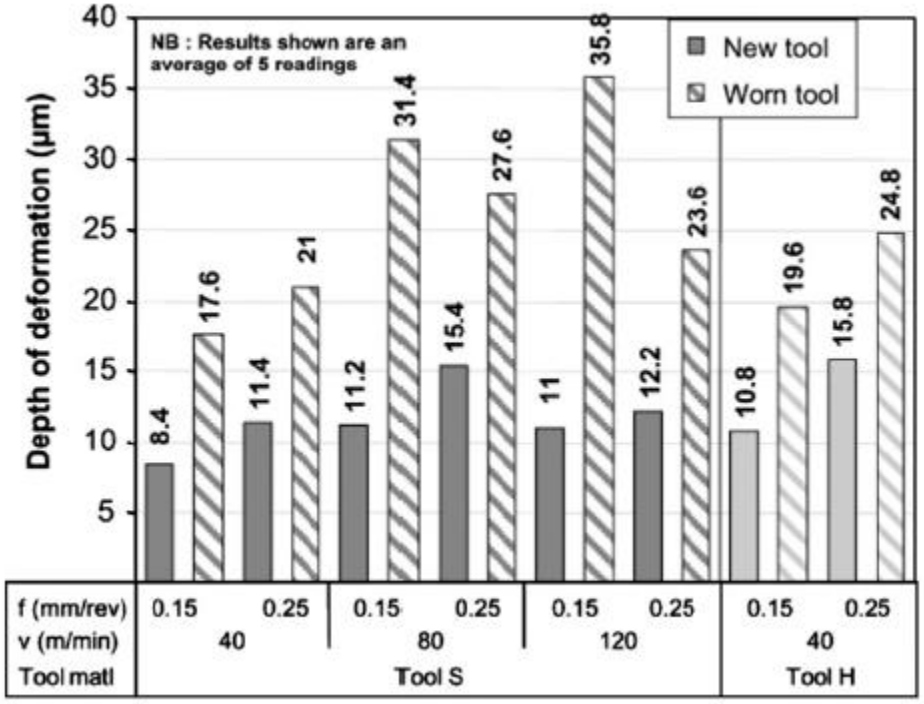

Fig. 10 Effect of new and worn out tools on SSD

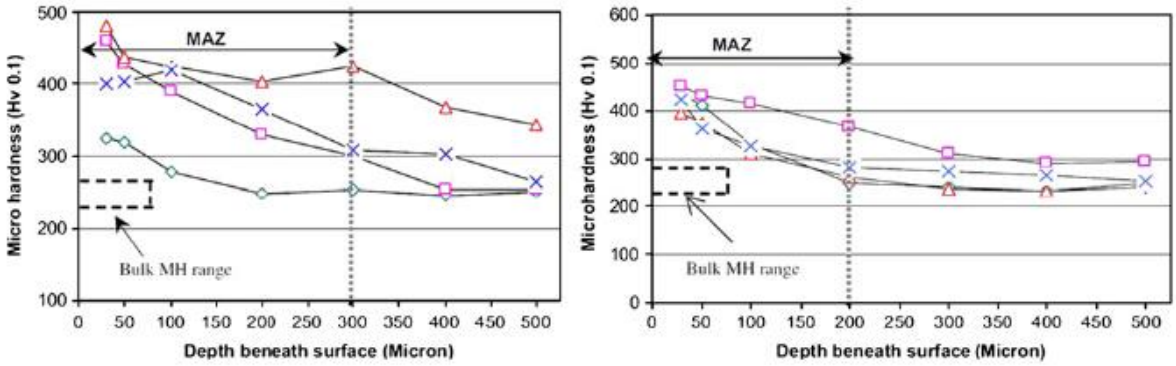

Fig. 11 The hardness profile of turned IN-718 at V=125-475 m/min, f=0.05-0.15mm/rev and DOC =0.5-1mm

Studies showed that both milling and turning produce hardened layer in machine effected zone as in fig.11. Hardened layer depend upon the machining parameters (feed rate, depth of cut and cutting speed), tool nose condition and material properties (thermal resistance, brittleness etc.).[6]

2.4 Cryogenic Machining effect on surface integrity

Pusaveca et al. studied the surface integrity in cryogenic machining of nickel alloys. Machining experiments were performed on Inconel 718 alloy used for the jet engines in the aerospace industry. Four samples were prepared: dry machining, minimum quantity lubrication, cryogenic machining (0.6kg/min/nozzle) and mixed (cryogenic and MQL). The turning experiments were conducted on the center less ground Inconel 718 round bars with a diameter of 32mm and length of 150mmin a CNClathe under constant cutting parameters: vc = 60m/min, f = 0.05 mm/rev, and ap = 0.63mm. Surface roughness was measured by non-contact interferometer profiler. [7]

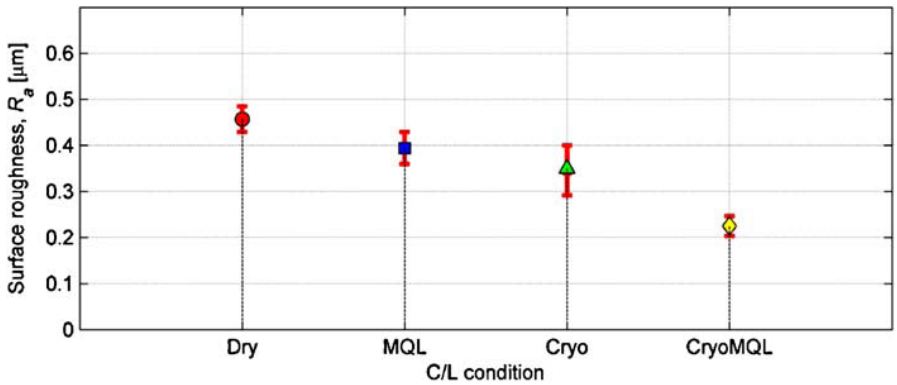

Fig. 12 Surface roughness at different conditions

Results showed that surface roughness of cryoMQL had minimum value means that gave the best surface finishing. However the forces for cryogenic machining is maximum as material surface frozen out before cutting that increased the hardness of material. Liquid nitrogen should be applied on cutting edge at time of cut. Subsurface damage and microstructure of different conditions were also studied.

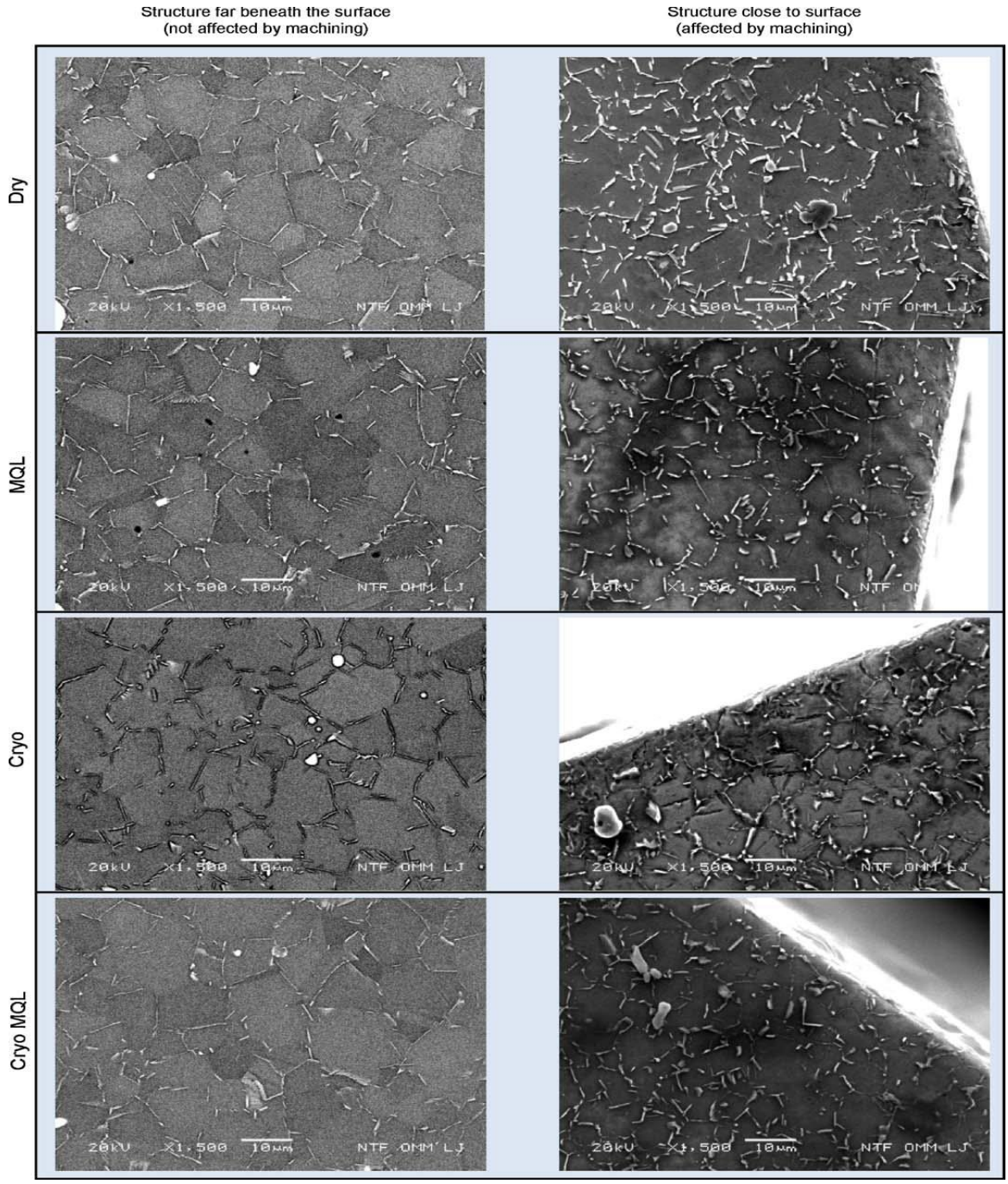

Fig. 13 SEM images of machine effected and non-effected by machining.

Results showed that work hardened is found 40 microns but it had decreasing trend in cryogenic machining. In SEM images, plastic deformation was also very low in depth about 1-2 microns in case of cryogenic machining.[7]

Ian S. Harisson et al. studied the effect of turning on different grades of steel. Three different grades of steels: 1053, 1070 and 51200 were tested. These samples were heat treated then hard turned on same conditions. Mounting, grinding, polishing and natal etching was carried out. Residual stresses, microhardness and white layer was measured.

Workpiece material:	52100
Cutting insert:	KD050
Speed:	300
Feed:	0.006

Tool life:	0%	14%	29%	43%	57%	71%	86%	100%
Measurement 1 [HRC]	63	63.1	58.6	61.6	59.6	57.5	57.6	53.9
Measurement 2 [HRC]	62.9	58.3	58.9	58.4	61.4	56.9	64.1	58.9
Measurement 3 [HRC]	64.3	59.4	62	60.3	61	59.1	61	60.4
Standard deviation	0.78	2.51	1.88	1.61	0.95	1.14	3.25	3.40
Avg	63.4	60.3	59.8	60.1	60.7	57.8	60.9	57.7

Fig. 14 Micro hardness at machining surfaces.

Results showed that hardness does not directly depends on the white layer formation and its thickness while the residual stresses had direct relation to the increase in hardness due to thermal gradient in machining process.[8]

2.5 Mechanical Parameters investigation of AISI 4340

Hassanpour et al. investigated the effect of milling parameters on the surface roughnes, micro hardness and white layer thickness formation. AISI 4340 material was heat treated and samples were prepared at different conditions. Portable roughness tester and V-test digital mciro hardness tester was used for surface roughness and micro hardness testing. Axial depth of cut, radial depth of cut, cutting speed and feed rate were the machining variables considered.

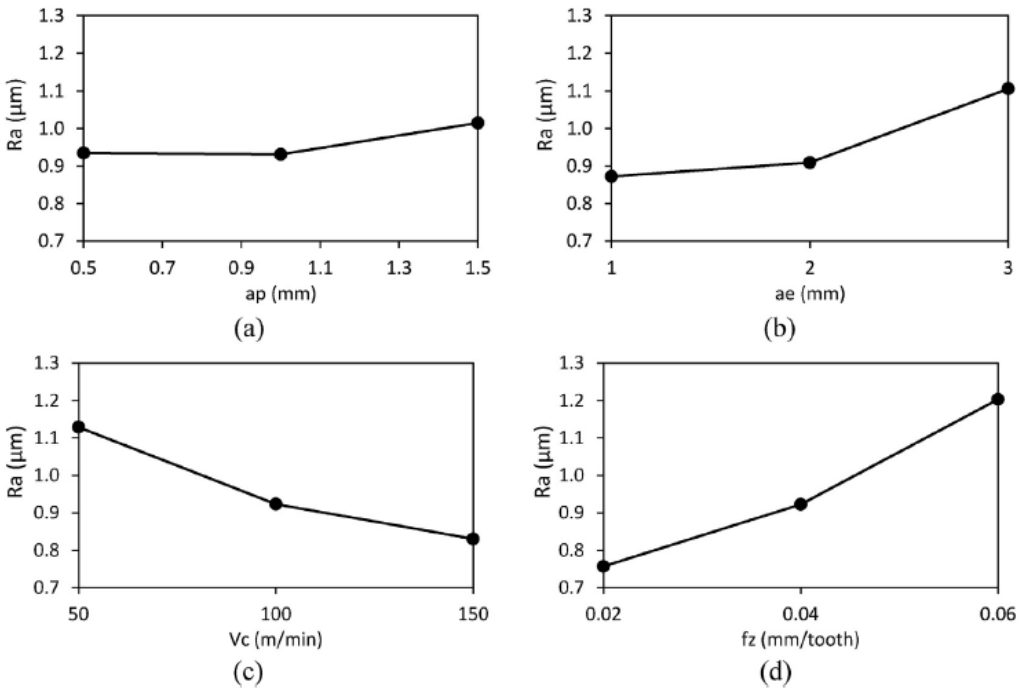

Fig. 15 Surface roughness vs cutting parameters a) Axial depth b) Radial depth c) cutting speed d) feed rate

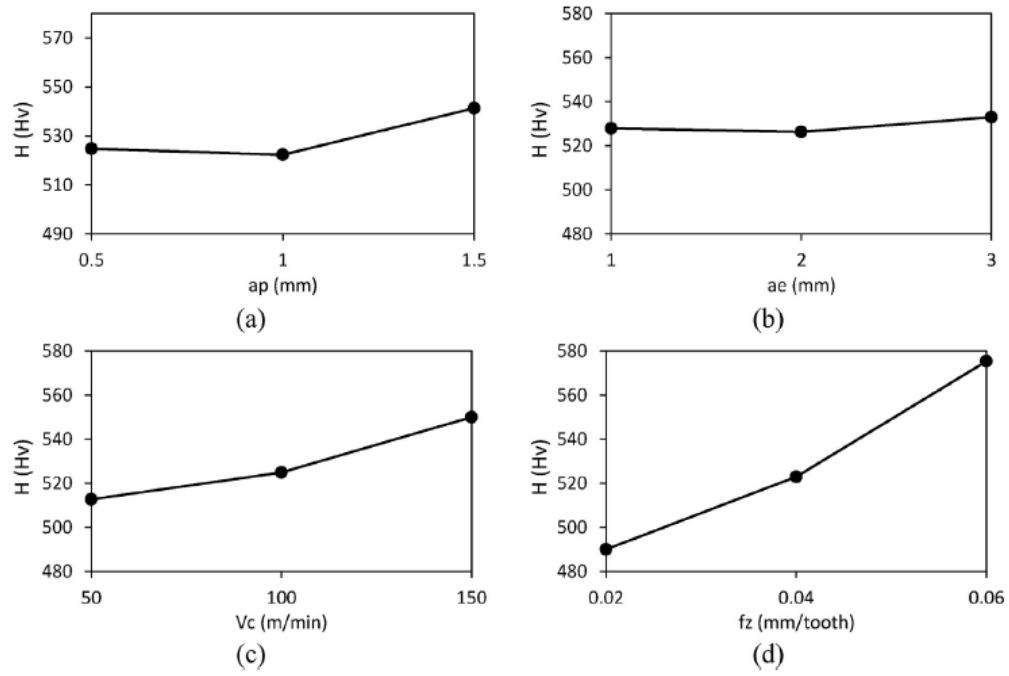

Fig. 16 Micro hardness vs cutting parameters a) Axial depth b) Radial depth c) cutting speed d) feed rate

Fig 15 and 16 shows the effect of each machining parameter on surface roughness and micro hardness. The analysis of variance showed that quadratic polynomial models estimate the surface roughness and micro hardness perfectly, while a linear model evaluate the variations of white layer thickness, as well. Feed rate had maximum effect on the surface roughness and micro hardness of hardened steel.[9]

2.6 Mechanical Characterization of friction stir welding of AA6061 and 6082

Imam Hejazi et al. studied the subsurface changes due to thermal stresses during friction stir welding in different regions in correlation with strength. AA6061 sample is used for stir friction welding. Sample was polished and etched with Keller`s reagent.

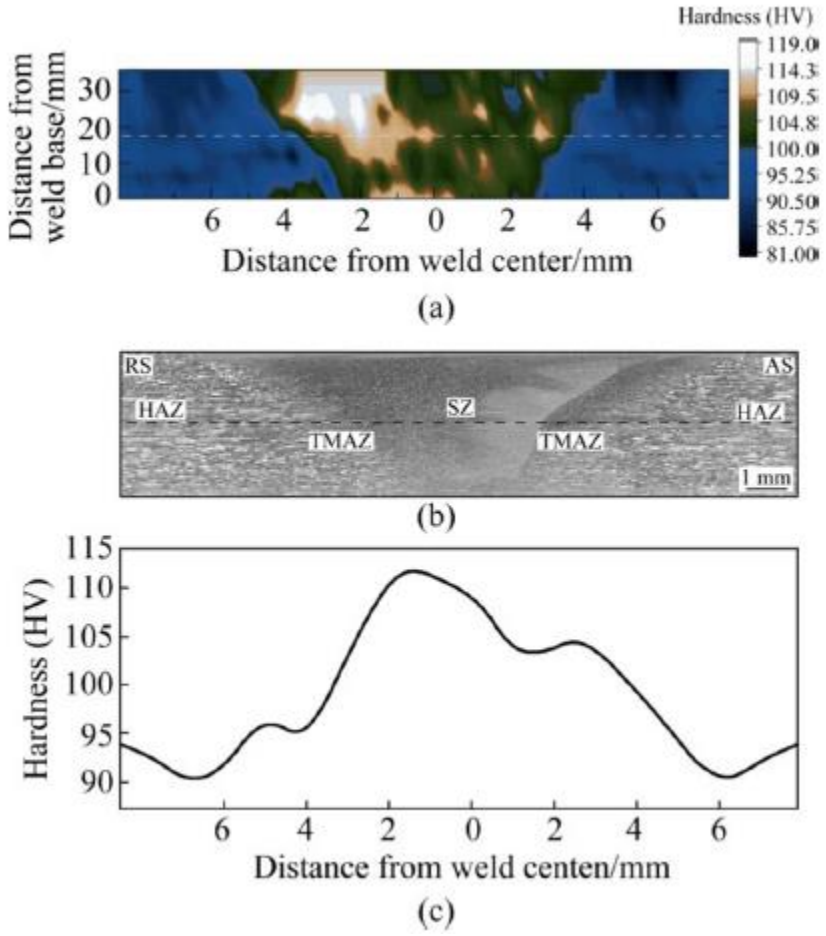

Fig. 17 Hardness map of FSW joint a) macro structure of welded samples b) its zones

c) Hardness profile line

Fig 17 shows the maximum hardness of HV 119 was obtained for the SZ, while the boundary between the HAZ and the TMAZ on the advancing side (failure location in the tensile

testing) exhibited the lowest hardness value of HV 81. It was shown that hardness mapping can be alternative for macroscopic in different situations. The investigation showed that hardness map is prediction of macroscopic and microscopic properties of FSW joints.[10]

Wan et al. studied the effect of friction stir welding on micro structure and micro hardness of Al-6082-T6 joints. Aluminum plates were used for experimentation and samples were prepared according to standard for macroscopic, microscopic and micro hardness inspection. Vickers hardness test was used for micro hardness values. At macroscopic level, different zones were identified.

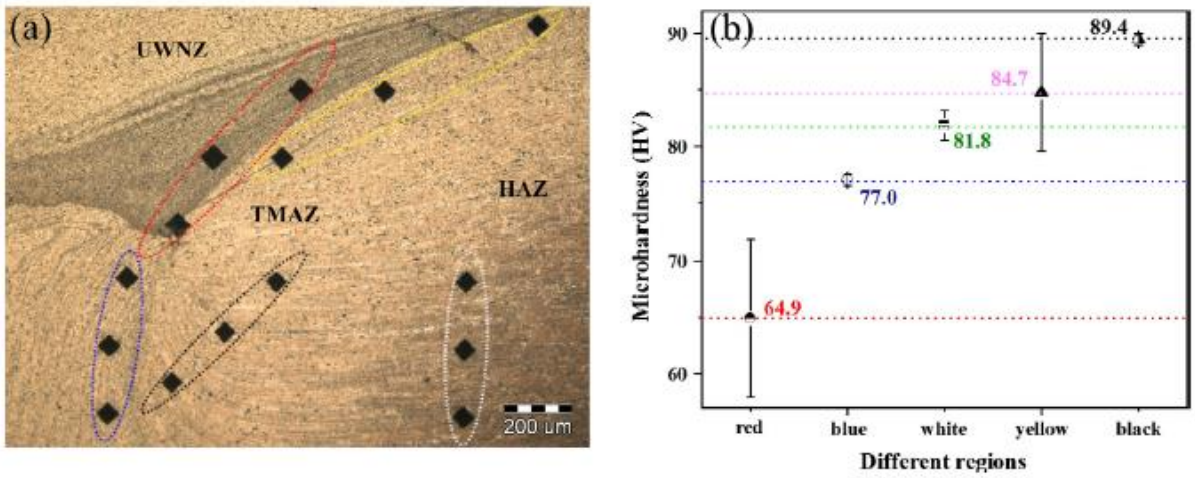

Fig. 18 a) micro hardness profile b) micro hardness values

The average micro hardness in the Weld Nugget Zone near the TMAZ was the lowest because of an over aging effect and the coarser second phase particles. The values of micro hardness of the TMAZ were relatively high which reached 89.4 HV and 84.7 HV, respectively. Thermal Machine Affected Zone had the most deformed structure while Heat Affected Zone had no prominent change in micro structure as compared to base material however grain size decreases with increase in distance from weld region.[11]

Sandeep Rathee et al. studied the optimized parameters for enhanced micro hardness of 6061/Sic surface composite fabricated via stir welding. Nine composite samples were prepared by changing the machining parameters; tool rotational speed, tool transverse speed and tilt angle. Micro hardness was measured by portable digital hardness tester.

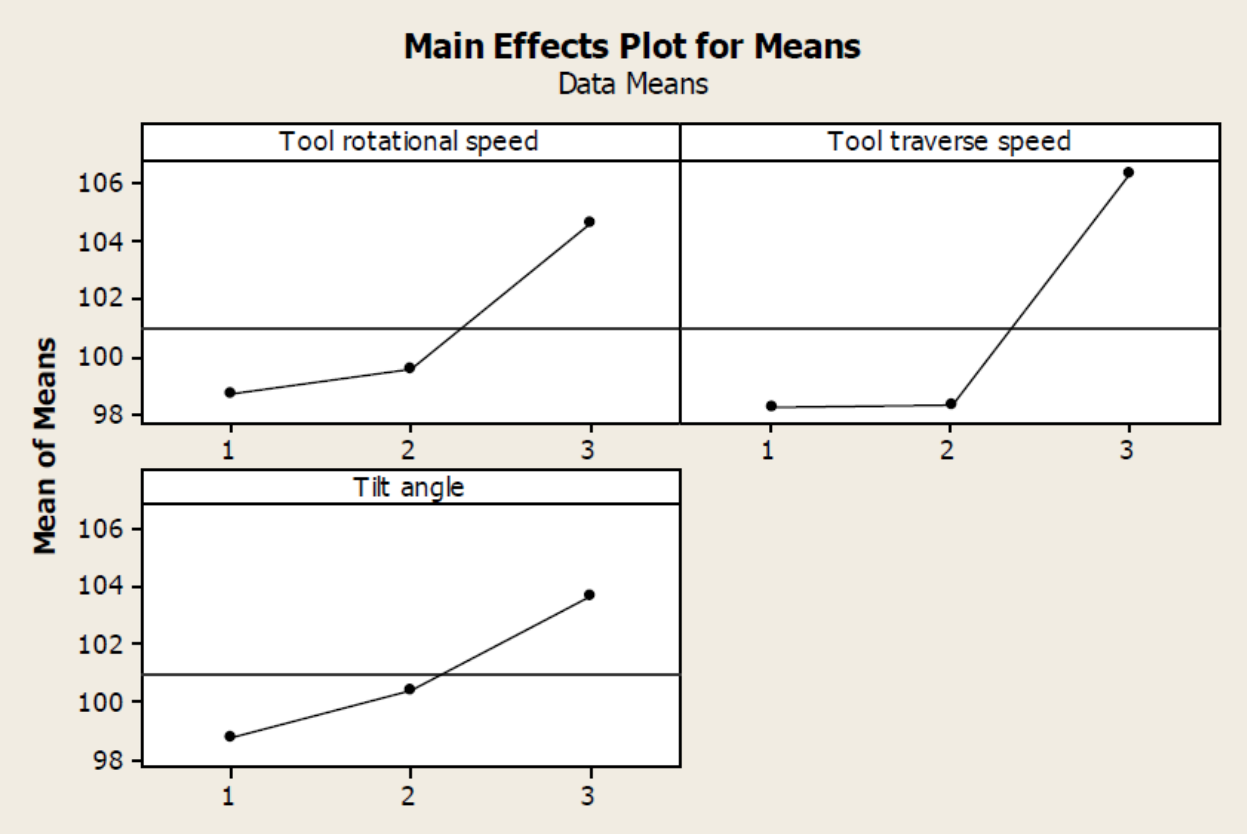

Fig. 19 Main effect plot of mean hardness values

Optimized values for hardness was tool rotational speed 1400rpm, tool transverse speed 50 mm/min, tool tilt angle of 2.5 degree respectively. Maximum hardness of 116 Hv was found at nugget zone as compared to base material hardness that was 94Hv average.[12]

2.7 Surface integrity of end milling

J. Sun et al. studied the effect of end milling on the surface and subsurface mechanical parameters on Ti-6Al-4V alloy at different machining conditions. Five levels of cutting speed, depth of cut and feed rate were selected. It was found that surface roughness had larger values in the direction of the cutting rather than feed direction.

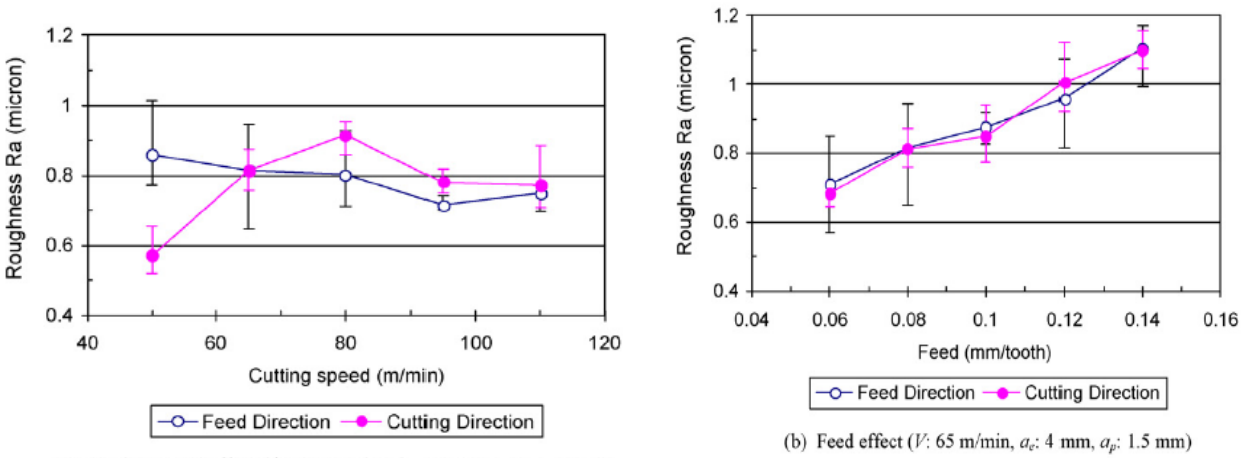

(a) Cutting speed effect (f: 0.08 mm/tooth, a_e: 4 mm, a_p: 1.5 mm)

(b) Feed effect (V: 65 m/min, a_e: 4 mm, a_p: 1.5 mm)

Fig. 20 influence of milling parameters on surface roughness a) cutting speed b) feed rate

It showed that feed rate had direct relation with the surface roughness while cutting speed relation was no obvious. Micro hardness was measured under the surface with Knoop micro hardness tester at pay load of 25gf.

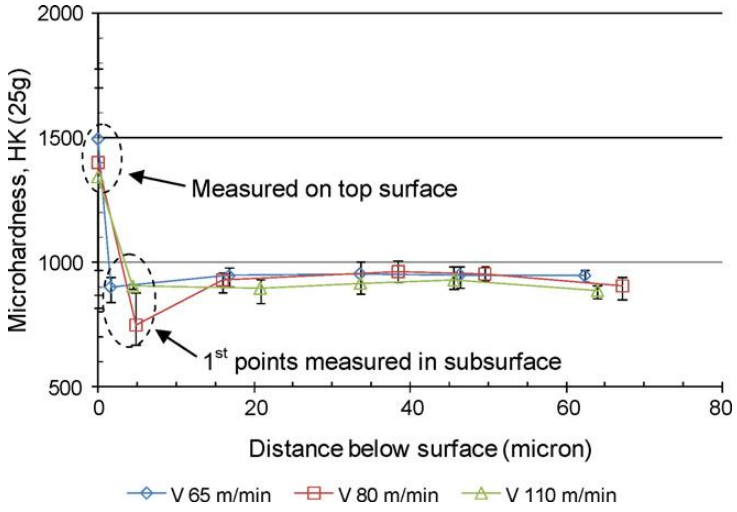

Fig. 21 Micro hardness distribution and variance in the subsurface (f=0.08mm/tooth, ae=4mm, ap=1.5mm)

Results showed that milled surface was of isotropic nature. Surface roughness value increases in cutting and feed direction with increase in feed and depth of cut, while increases in cutting direction at low speed and decreases at high speeds. Surface roughness decreases in feed direction with cutting speed.[13]

Jian Wang et al. evaluated the subsurface damage in optical glass. It was found that hardness decreases with the distance from the edge of the glass. It was studied by different author and is useful technique to analyze the sub surface damage.[14]

L.C. Lee et al. studied the subsurface damage of steel tools after EDM. Samples were prepared at variable current and pulse time. Surface roughness was measured by taly surf stylus and subsurface damage by Scanning Electron Microscope. Thickness of white layer was termed as subsurface damage is directly proportional to the pulse energy. Surface roughness was greatly depends upon the pulse current and pulse energy in a specified relation. Surface roughness and white layer formation was independent of the type of steel used as thermal property of solidifying material is not depend on these parameters.[15]

M-B. Mhamdia et al. studied the surface integrity of Ti-6Al-4V material at different milling parameters. Material was milled at different angles and feed rates. Surface roughness was measured by 3-D roughness tester and vicker micro hardness tester was used for micro hardness and these results were compared with micro structural results by SEM.

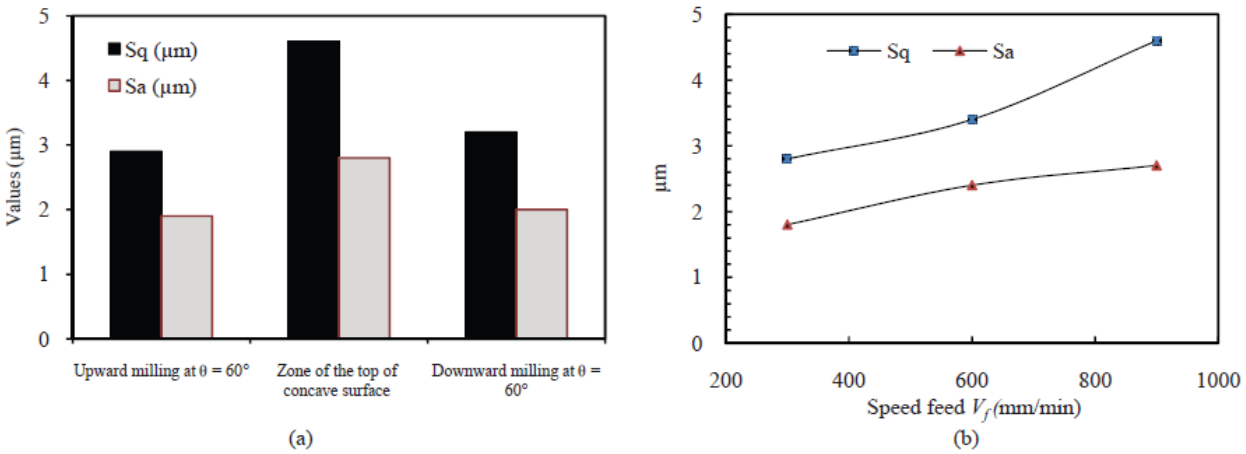

Fig. 22 The variation of Sa and Sq a) at tool position at N = 3000 rpm, *Vf* = 900 mm/min, ae = 0.5 mm, ap = 0.5 mm b) at feed speed *Vf* at N = 3000 rpm, ae = 0.5mm, ap = 0.5 mm.

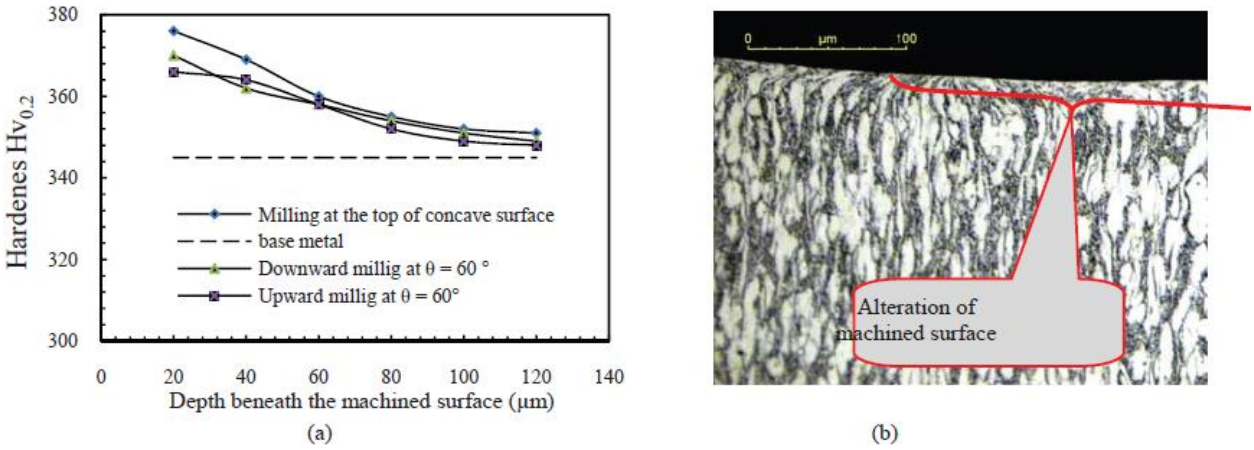

Fig 23 a) Microstructure micro hardness profile from machine distance b) micro structure alteration from top side

Results showed that surface finish was effected by the position of the tool, at upward and downward milling it gave best surface finish as compared to top concave surface. Plastically deformed layer was formed shown by micro hardness neither by heat effected zone nor by white layer thickness, it was also effected by tool position.[16]

Nancy M. McCurry et al. studied the temperature resistance coefficient relationship with the grain boundaries. Aluminum samples were prepared at different temperatures and were studied under SEM. Results showed that grain size increased with increase in temperature deposition. Change in size of grains was more when heated up to 200ºC than heated to 400ºC. Although the size of grain at 200ºC was less than that at 400ºC.[17]

2.8 Subsurface deformation in machining of Inconel 718

Jimmig Zhou et al. studied the subsurface damage in cutting of Inconel 718 at four different feed rate, three cutting speed and single depth of cut conditions. Two type of tools, semi worn out and worn our tools were used.

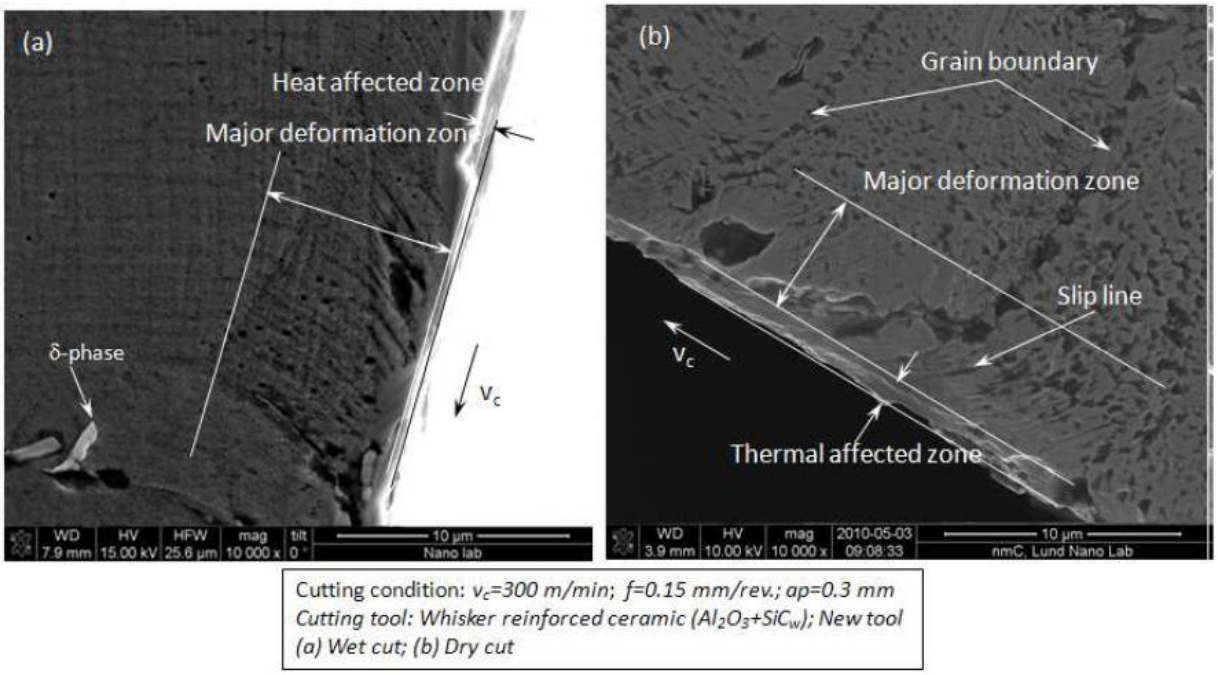

Fig. 24 Morphology of subsurface damage under HRSEM

Fig. 24 showed that worn out tool at dry condition had maximum damage to the subsurface and plastic deformation region is high as compared to semi-worm out dry and wet conditions.

Micro hardness test was carried out with the increment of 10 microns in depth. It reveals the micro hardness values under different cut condition. The increase of micro hardness values in the dry cut was found smaller than wet cut condition when the same cutting parameters were employed although larger strain of grains were observed in the near surface region.

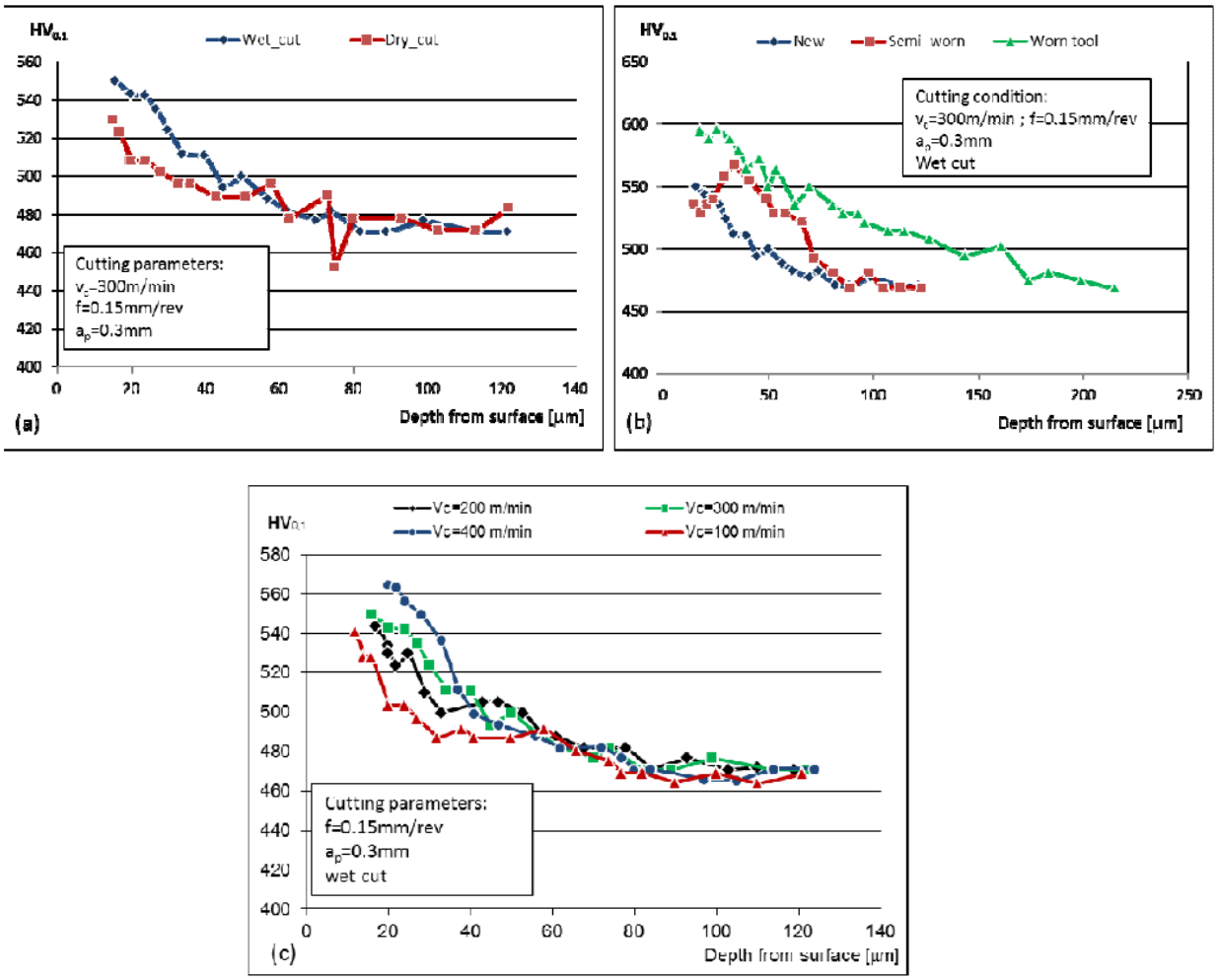

Fig 25. Micro hardness on deformed layer

Fig. 25 showed that dry cut does not produce significant difference of micro hardness in the subsurface layer, it has, however, profound reduction in tool life. Value of hardness was greater near machine affected zone due to thermal and residual stresses.[18]

2.9 Subsurface and surface roughness comparison of ground optical materials

Li Sheng et al. studied the grinding effects on subsurface damage to surface roughness ratio. Several BK7 glass samples were prepared in order to analyze the effect of grinding. Round indenter was used to determine micro hardness under the surface. SSD depth of 80 grit and 120 grit BK7 glasses were 52.9µm and 38.0µm respectively.

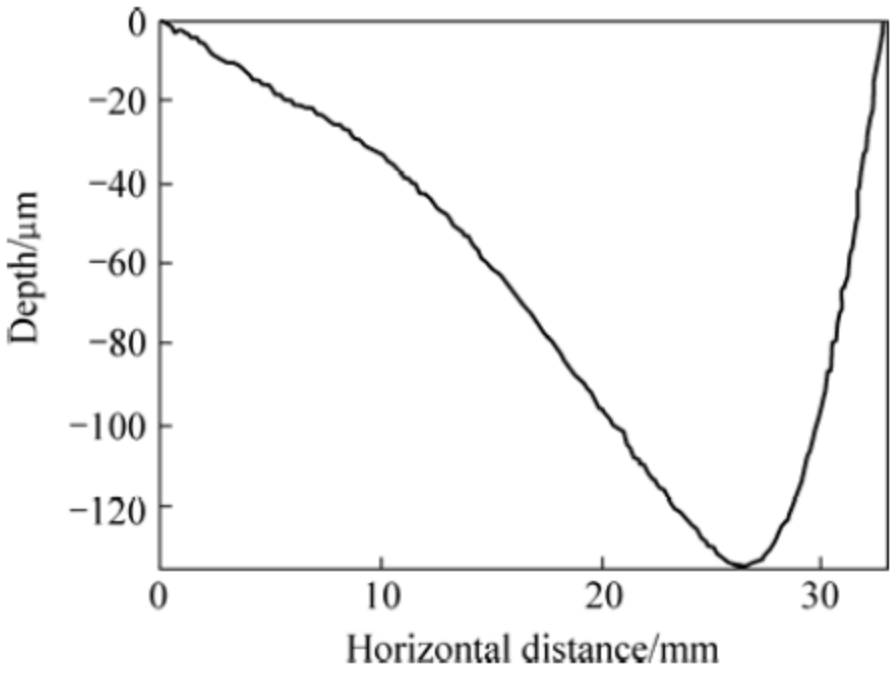

Fig. 26 Depth profile across centerline

Results showed that SSD/SR ratio of ground optical materials can be effectively predicted by material mechanical properties, geometrical properties and load of abrasive grains. The SSD/SR ratio is directly proportional to load of abrasive grains, while inversely proportional to granularity of abrasive grains, especially. Mechanical properties of material affect SSD/SR ratio severely.[19] Meenu Gupta et al. studied the comparison of surface roughness and material removal rate in turning of UD-GFRP. Samples were prepared on turning machine by changing tool parameters (Tool nose radius and tool rake angle) and machining parameters (speed of cut, feed rate, coolant ratio and depth of cut).

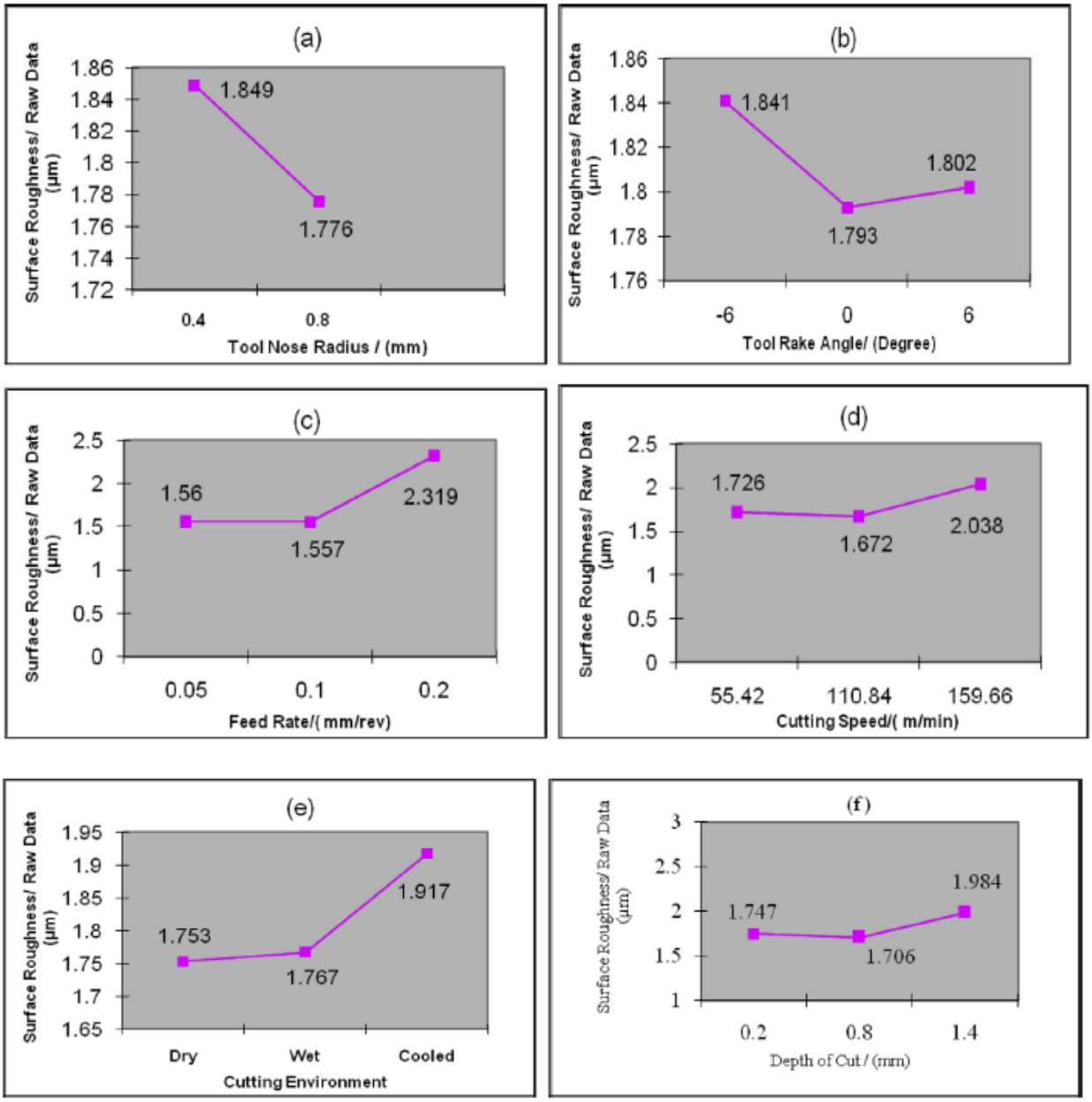

Fig. 27 Response graphs of surface roughness

Results showed that feed rate was the most influential parameter as compared to other machining parameters (depth of cut and speed of cut).[20]

2.10 Micro hardness comparison with strength of Al-7010

M. Tiryakioglo et al., studied the effect of strength by changing the micro hardness of material having same chemical composition. Samples of Aluminum for tensile testing was

prepared from forged material. These samples were heated and quenched at different condotions to vary the hardness values. Equations that relates yield stress with hardness is as follows:

$$\sigma_Y = \frac{H_V}{0.927C}$$

and

$$\sigma_Y = \beta_1 H_V + \beta_0$$

Where C=2.956, β_1= 0.268~0.39, β_0= slope of the stress and hardness curve.

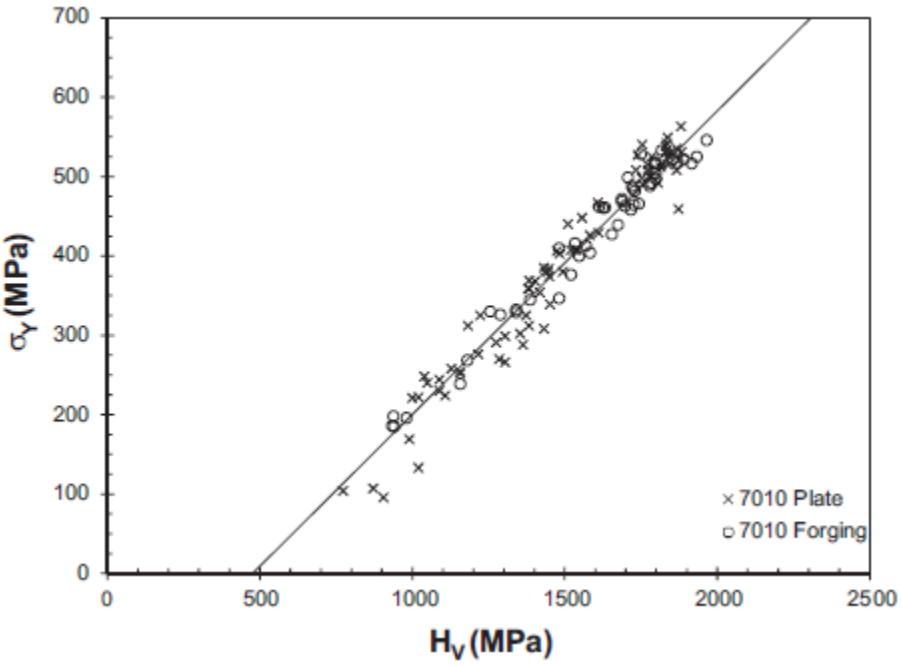

Fig. 28 Yield stress vs vicker hardness for 7010 plate and forging studied.

It was concluded that vicker hardness-Yield stress relationship for 7010 was developed:

$$\sigma_Y = 0.383H_V - 182.3$$

That data from two independent studies using the aluminum alloy 7010 overlapped was quite significant and indicated a fundamental relationship between hardness and strength. The same fit to both data sets also provided a very respectable fit to a third independent study.[21]

2.11 Prediction of subsurface damage depth by surface profiling

Tsutomu ohta et al. related the surface roughness of brittle material (optical grade germanium and silicon) after grinding at different parameters to the subsurface cracks growth.

Germanium and silicon samples were grinded at four different grinding parameter (changing abrasive size). Surface roughness was studied by contact stylus.

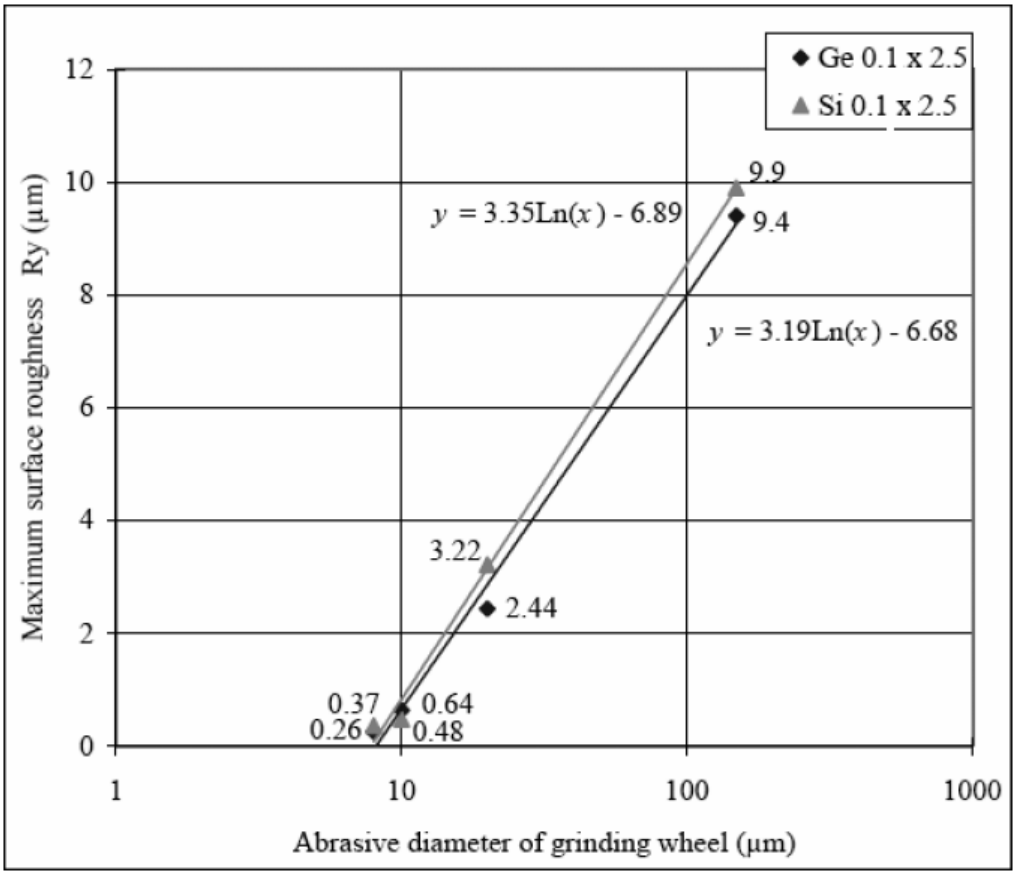

Fig. 29 Surface roughness measured by Talystep with the 0.1 × 2.5 µm rectangular stylus

For silicon,

$$y = 3.35\mathrm{Ln}(x) - 6.89$$

For Germanium,

$$y = 3.19\mathrm{Ln}(x) - 6.68$$

These relations showed that surface roughness was directly affected by abrasive diameter. For subsurface crack detection, small polishing method and slanted polishing method was used in small polishing method surface was polished finely then stylus was employed to measure the shallowness of the crack.

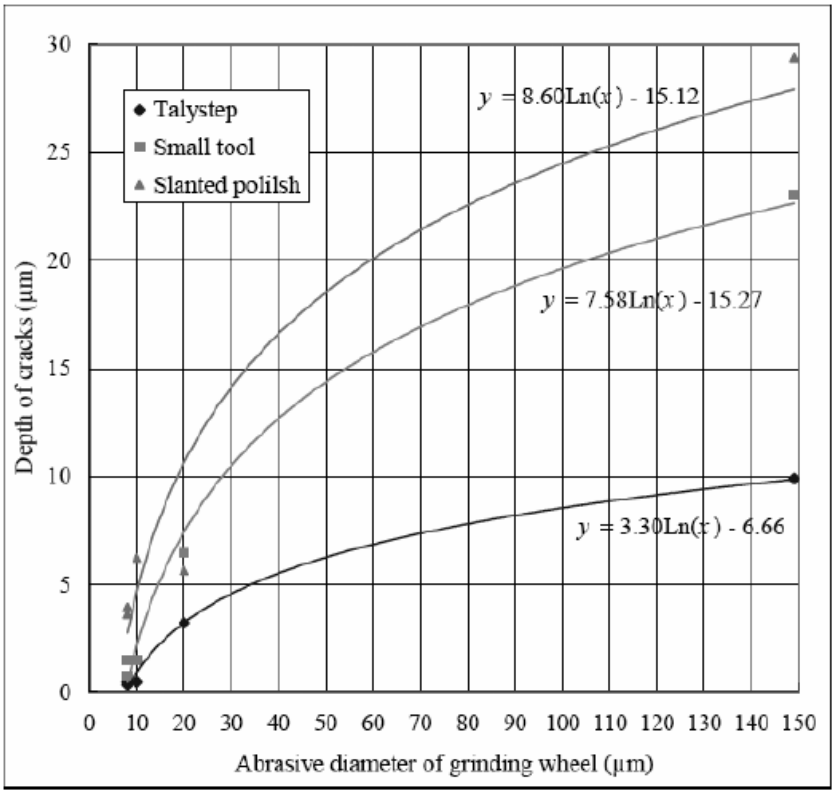

Fig. 30 Graph of crack depth by two different methods

Results showed that surface roughness had logarithmic relationship with abrasive diameter. Small tool polishing with fine silica abrasives was much effective. Silicon and germanium both had similar subsurface damage depth.[22]

2.12 Effect of temperature on subsurface microstructure of Al 7075

Omar Fergania et al. studied the effect of turning on microstructure and micro hardness of aluminum 7075. Three samples of variable depth of cut were prepared for the analysis of micro hardness using micro hardness tester. Grain size along the boundary and micro hardness was studied.

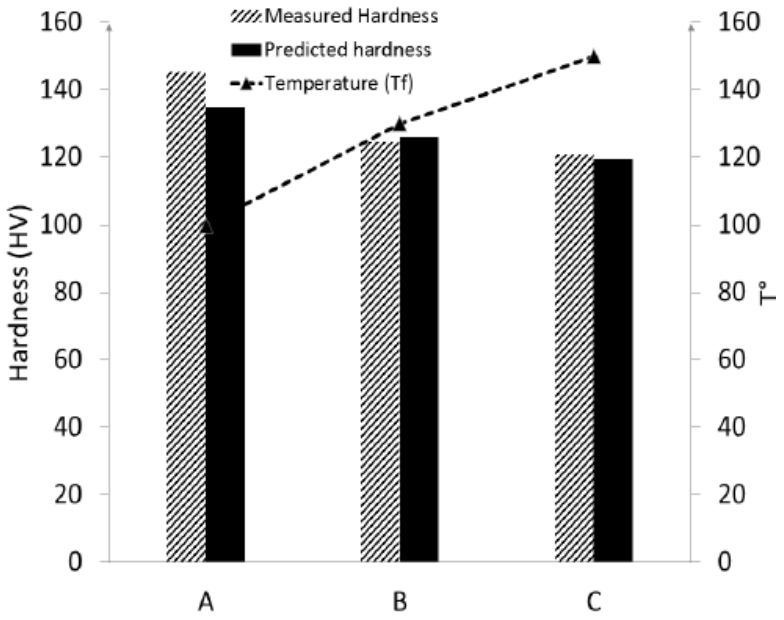

Fig. 31 Graph of hardness vs samples for sample A, d=0.1mm, for B, d=1mm, for C, d=2.0mm

Predicted hardness was calculated from Hall-Petch Relation. Results showed that increasing the depth of cut it resulted in increase in grain size that reduced the micro hardness values beneath the surface.[23]

2.13 Effect of torsion on micro hardness of Al-6061 composite

Saleh N. Alhajeri et al. studied the micro structure and micro hardness of Al-6061 metallic composite with 10% Al_2O_3 particles subjected to torsional loading. 60 GPa torsional load was applied on the sample. Sample was prepared for metallography by mounting, grinding and polishing. Sample was processed for 10 turns and effect of these turns were checked at several points during processing.

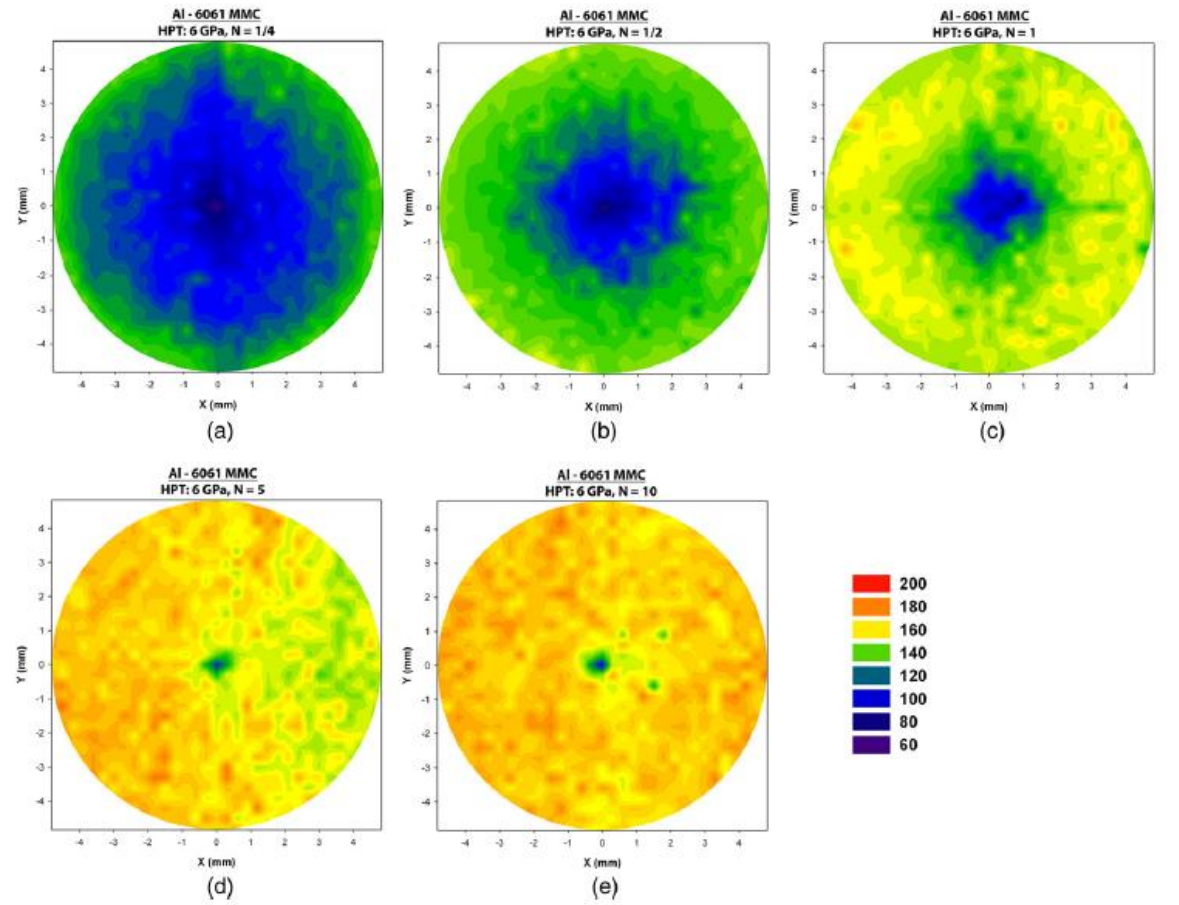

Fig. 32 Color coded graphs of micro hardness a)1/4, b)1/2, c)1, d)5 and e) 10 turns

Results showed that micro hardness increases linearly with the fraction of number of turns (<1) from 62 Hv to ~140 Hv near edge. While at large number of turns N=10 hardness became more saturated of ~170 at outer region.[24]

2.14 Summary of Literature Review

Sr. No.	Authors	Journal/ Conference	Conclusion
1.	S. Missori and A.Silli	Dipartimento Chimica Industriale e Ingegneria dei Materiali - Università di Messina - Italy	Welded material fracture earlier than un welded material. In HAZ, both hardness and tensile strength reduce to its minimum value and SEM images shows that during fatigue life testing most samples fails in HAZ
2.	BLAINEAUA, R. LAHEURTEA, P. DARNISA, N. DARBOISA, O. CAHUCA, J. NEAUPORT	21ème Congrès Français de Mécanique	Fraction of valley roughness profile (100-Mr2), calculated by Abbot-Firestone curve, is in linear relationship SSD and is more accurate indicator than maximum peak to valley roughness (Rt max)
3.	DOBRESCU, Tiberiu, Gabriel; PASCU, Nicoleta - Elisabeta; OPRAN, Constantin & BUCURESTEANU, Anca Monica	Proceedings of the 23rd International DAAAM Symposium	Penetration depth of subsurface damage depends on ceramic type, Brittleness and maximum grit of depth of cut.
4.	Durul Ulutan, Tugrul Ozel	International Journal of Machine Tools & Manufacture	Both milling and turning produce hardened layer in machine effected zone. Hardened layer depend upon the machining parameters (feed rate, depth of cut and cutting speed), tool nose condition and material properties (thermal resistance, brittleness etc.)

5.	F. Pusaveca, H. Hamdib, J. Kopaca, I.S. Jawahirc	Journal of Materials Processing Technology	Surface roughness of cryo MQL had minimum value means that gave the best surface finishing. However the forces for cryogenic machining is maximum as material surface frozen out before cutting that increased the hardness of material. Liquid nitrogen should be applied on cutting edge at time of cut.
6.	Hassanpour, Hamed Sadeghi, Mohammad H. Rasti, Amir Shajari, Shaghayegh	Journal of Cleaner Production	Quadratic polynomial models estimate the surface roughness and micro hardness perfectly, while a linear model evaluate the variations of white layer thickness, as well. Feed rate had maximum effect on the surface roughness and micro hardness of hardened steel
7.	Iman HEJAZI, Seyyed Ehsan MIRSALEHI	Trans. Nonferrous Met. Soc. China	The maximum hardness of HV 119 was obtained for the SZ, while the boundary between the HAZ and the TMAZ on the advancing side (failure location in the tensile testing) exhibited the lowest hardness value of HV 81. It was shown that hardness mapping can be alternative for macroscopic in different situations. The investigation showed that hardness map is prediction of macroscopic and microscopic properties of FSW joints.
8.	Long Wan, Yongxian Huang , Zongliang, Shixiong , Jicai Feng	Materials and Design	Thermal Machine Affected Zone had the most deformed structure while Heat Affected Zone had no prominent change in micro structure as compared to base material however grain size decreases with increase in distance from weld region.

9.	Sandeep Rathee, Sachin Maheshwari, Arshad Noor Siddiquee, Manu Srivastava1, Satish Kumar Sharma	Materials Today: Proceedings	Optimized values for hardness was tool rotational speed 1400rpm, tool transverse speed 50 mm/min, tool tilt angle of 2.5 degree respectively. Maximum hardness of 116 Hv was found at nugget zone as compared to base material hardness that was 94Hv average
10.	J. Sun, Y.B. Guo∗	Journal of Materials Processing Technology	Milled surface was of isotropic nature. Surface roughness value increases in cutting and feed direction with increase in feed and depth of cut, while increases in cutting direction at low speed and decreases at high speeds. Surface roughness decreases in feed direction with cutting speed.
11.	Jian Wang,Yaguo Li,Jinghua Han,Qiao Xu,Yinbiao Guo	Journal of the European Optical Society	It was found that hardness decreases with the distance from the edge of the glass. It was studied by different author and is useful technique to analyze the sub surface damage.
12.	L. C. LEE, L. C. LIM, V. NARAYANAN and V. C. VENKATESH	International Journal of Machine Tools & Manufacture	Surface roughness was greatly depends upon the pulse current and pulse energy in a specified relation. Surface roughness and white layer formation was independent of the type of steel used as thermal property of solidifying material is not depend on these parameters.
13.	M-B. Mhamdia, M. Boujelbenea,, E. Bayraktara, A. Zghalb	Physics Procedia	Surface finish was effected by the position of the tool at upward and downward milling it gave best surface finish as compared to top concave surface. Plastically deformed layer was formed shown by micro hardness neither by heat effected zone nor by white layer thickness, it was also effected by tool position

14.	Jinming Zhou,, Volodymr Bushlya, Ru Lin Peng and Jan-Eric Stahl	Applied Mechanics and Materials	Dry cut does not produce significant difference of micro hardness in the subsurface layer, it has, however, profound reduction in tool life. Value of hardness was greater near machine affected zone due to thermal and residual stresses
15.	M. Tiryakioğlu,n, J.S.Robinson, M.A.Salazar-Guapuriche, Y.Y.Zhao, P.D.Eason	Materials Science & Engineering	Data from two independent studies using the aluminum alloy 7010 overlapped was quite significant and indicated a fundamental relationship between hardness and strength. The same fit to both data sets also provided a very respectable fit to a third independent study.
16.	Tsutomu Ohta	International Journal of Machine Tools & Manufacturing	Surface roughness had logarithmic relationship with abrasive diameter. Small tool polishing with fine silica abrasives was much effective. Silicon and germanium both had similar subsurface damage depth
17.	Omar Fergania, Yamin Shaoa, Steven Y. Lianga	2nd CIRP 2nd CIRP Conference on Surface Integrity (CSI)	Predicted hardness was calculated from Hall-Petch Relation. Results showed that increasing the depth of cut it resulted in increase in grain size that reduced the micro hardness values beneath the surface
18.	Saleh N. Alhajeri , Khaled J. Al-Fadhalah, Abdulla I. Almazrouee, Terence G. Langdon	Materials Characterization	Results showed that micro hardness increases linearly with the fraction of number of turns (<1) from 62 Hv to ~140 Hv near edge. While at large number of turns N=10 hardness became more saturated of ~170 at outer region.

Table 01 Summary of literature review

Chapter 3: Design of Experiment, Sample Preparation and Experimental Setup

3.1 Selection of Material

Material used for machining and studying the effect on surface roughness, subsurface damage and fatigue life is aerospace grade aluminum 6082-T6 alloy. T6 indicates that it is artificially aged aluminum alloy. Composition test was conducted having the composition as follows:

Element	Composition (%)
Al	Balance
Zn	0.37
Si	0.35
Mn	0.85
Mg	0.64
Fe	0.4
Cu	4.56
Ti	-
Cr	-

Table 02 Al-6082 Material composition

3.2 Dimensions of specimen

Dimensions are selected as per ISO 1143:2010 standard for fatigue testing. For turning for comparison same dimensions are adopted as per fig given below.

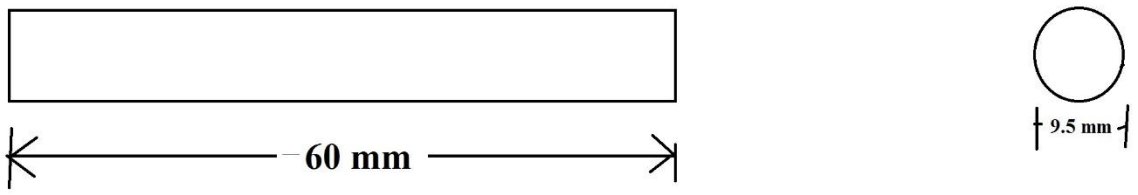

Fig. 28 Dimensions for turning specimen.

3.3 Selection of Insert and Shank

For the selected machining parameters and material, shank and insert was selected from the Sandvik Coromat catalogue 2011 for the single point turning of Aluminum 6082-T6. The codes for insert and shank were VCGX 16 04 04-AL H10 and SVVBN 2525M 16 resepectively.

3.4 Input and Response Variables

3.4.1 Input Variables:

Input variables are selected as prescribed by the catalogue of tool manufacturer that is Sandvik Coromat catalogue 2011 and ISO 3685 standard for the "Tool-life testing with single-point turning tool". Input variables for turning of material are:

- Feed rate (0.15, 0.2, 0.25 mm/rev)
- Cutting speed (1500rpm (44.77m/min), 2000rpm (59.69 m/min), 2500rpm (74.613 m/min))
- Depth of cut (1.25, 1.5, 1.75 mm)

3.4.2 Responsible Variables:

Response variables selected for this research are:

- Surface Roughness
- Sub surface Damage
- Fatigue life comparison.

3.5 Design of Experiment

Sample preparation was conducted by changing the combination of different machining parameters as specified by input parameters of all three parameters and their values. Full factorial approach was used to test all possible combinations of parameters and their ranges. List of samples prepared for analysis is as follows:

Sr. no.	Feed rate (mm/rev)	Cutting Speed (rpm)	Depth of cut (mm)
1	0.15	1500	1.25
2	0.15	2000	1.25
3	0.15	2000	1.5
4	0.15	2000	1.75
5	0.15	2500	1.5
6	0.15	2500	1.75
7	0.2	1500	1.25
8	0.2	1500	1.5
9	0.2	2000	1.25
10	0.2	2000	1.75
11	0.2	2500	1.5
12	0.25	1500	1.5

13	0.25	2000	1.5
14	0.25	2000	1.75
15	0.25	2500	1.5
16	0.25	2500	1.75
17	0.25	1500	1.25
18	0.2	2500	1.75
19	0.2	1500	1.75
20	0.15	2500	1.25
21	0.2	2500	1.25
22	0.25	2000	1.25
23	0.25	2500	1.25
24	0.15	1500	1.5
25	0.2	2000	1.5
26	0.15	1500	1.75
27	0.25	1500	1.75

Table.03 Design of experiment

3.6 Machining Procedure

Aluminum rods of 20 mm diameter and length of 1 meter in length are cut into length of above mentioned length with the help of SiC water cooled cutter. Diameter of the samples are reduced to 9.5mm as prescribed by ISO 1143:2010 for fatigue testing specimen preparation at different machining conditions as in above mentioned table for machining samples. Turning of samples are carried on multiple tool turret CNC lathe machine model ML-300 having maximum spindle speed of 3500rpm. Each insert is used for the machining of 3 samples while insert 6, 7 and 8 is used for the machining of four samples.

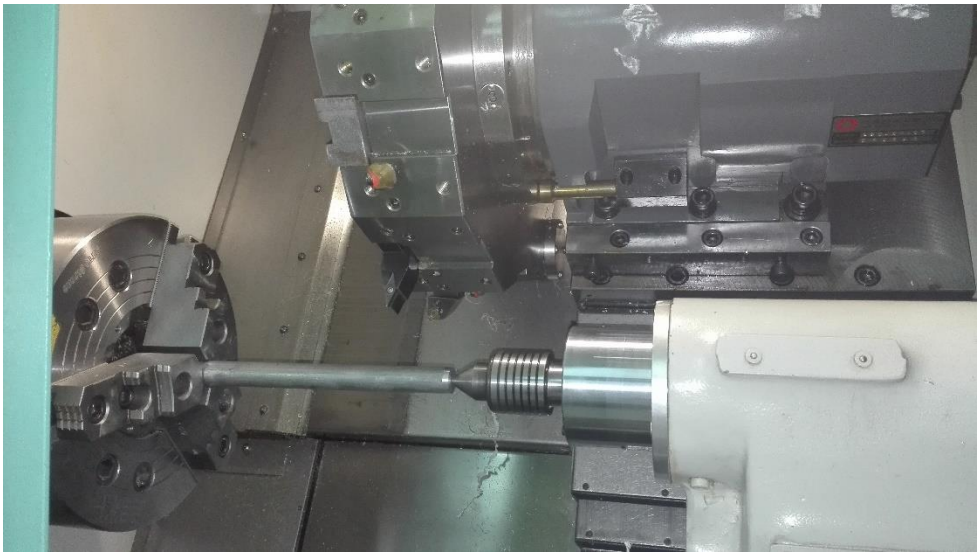

Fig. 29 CNC Lathe machine, sample preparation

3.7 Sample Preparation for Metallography

3.7.1 Sectioning of samples

Machined samples are sectioned for microscopic study from the long machined rods. 5mm sample length sample is cut with the help of SiC 20 grit saw with continuous cooling of water to avoid any deformation in grain structure and upper layer of the sample. 10-15 μm of space is to be spared from both ends to compensate the effects of cutting.[25]

3.7.2 Mounting of Samples

Mounting of samples are necessary to hold them for grinding, polishing, stabilizing the foundation of the sample and provide edge retention. For that purpose, 27 samples are hot mounted using bakelite powder as the base. For comparison of change in mechanical properties of samples, 3 samples are cold mounted. For hot mounting, Hydropress automatic mounting machine is used. For cold mounted samples, acrylic solution with fast hardener is used.

Sr. No.	Parameter	Value
1.	Temperature	114°C
2.	Pressure	280 Bar
3.	Settling Time	4 min

Table. 04 Parameters for hot mounting.

a) b)

Fig 35 a) hot mounted sample, b) hot mounting machine

3.7.3 Grinding of Samples

Reflecting surface is needed for conducting hardness test, for that purpose grinding of samples for fine surface finish is followed. This process is completed in five steps using different SiC sand papers of different grit sizes. Metkon Gripo 2V grinder polisher machine is used at speed of 600-800 rpm. Different grit size sand papers used are: 120, 320, 800, 1200 and 2000 to achieve the finner surface. Direction of cut is changed to 90° for every step of the grinding. Water is constantly splashed to avoid the increase in temperature. [26]

Fig.36 Metkon Gripo 2V grinding and polishing machine

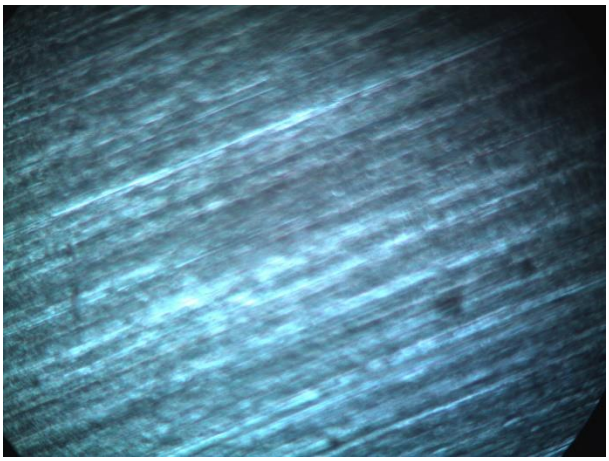

(a)

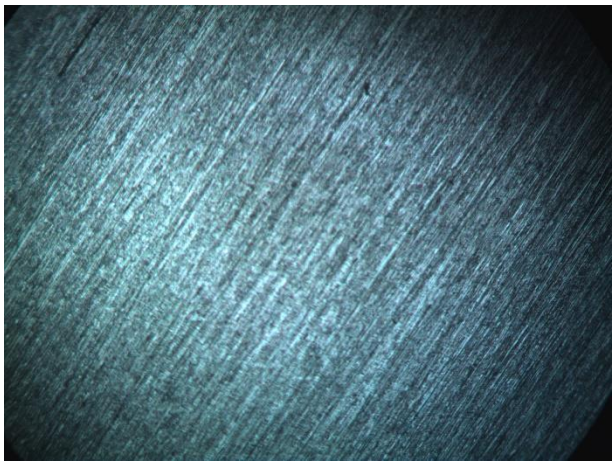

(b)

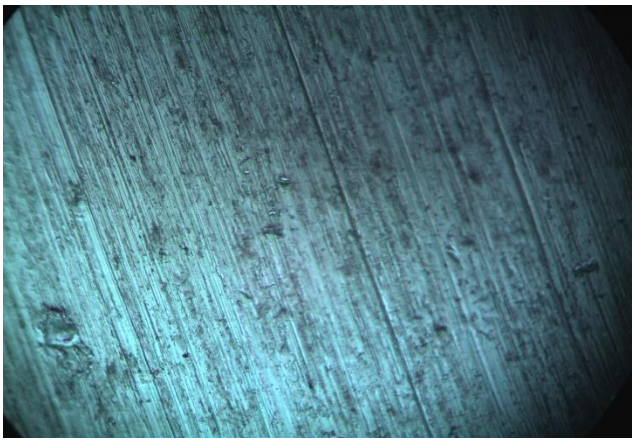

(c)

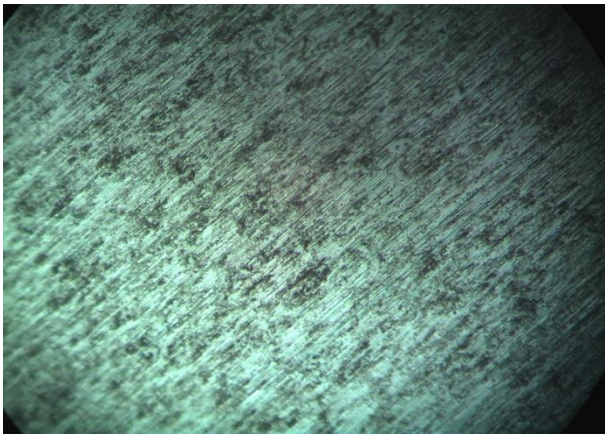

(d)

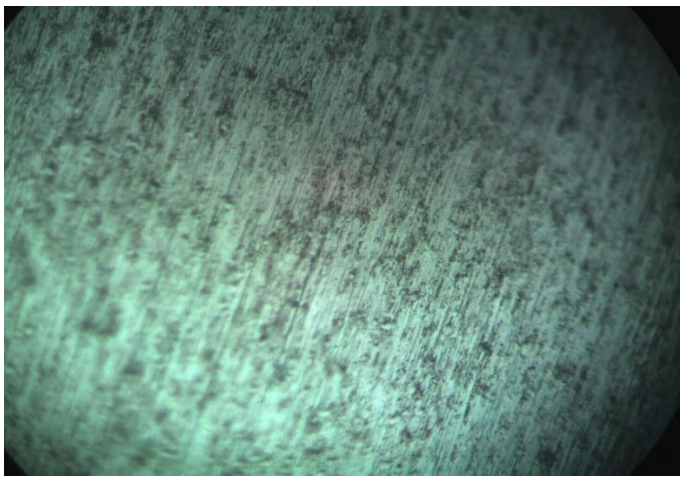

(e)

Fig.37 Grinding images of sample at; FR= 0.15mm/rev, CS=2000 and DoC= 1.5mm at 500X a) 120, b)320, c)800, d)1200, e)2000 grit

3.7.4 Polishing of Samples

For fine mirror like surface after grinding to smooth surface polishing is required. Polishing is carried out at different stages using diamond paste of different particle size at 6μm, 3μm, 1μm and 0.1μm with diamond lubricant. Finest surface is achieved from 0.05μm alumina colloidal solution. Sample is rotated through the paper. Sample surface gets finer with reducing the grain size of the diamond paste.

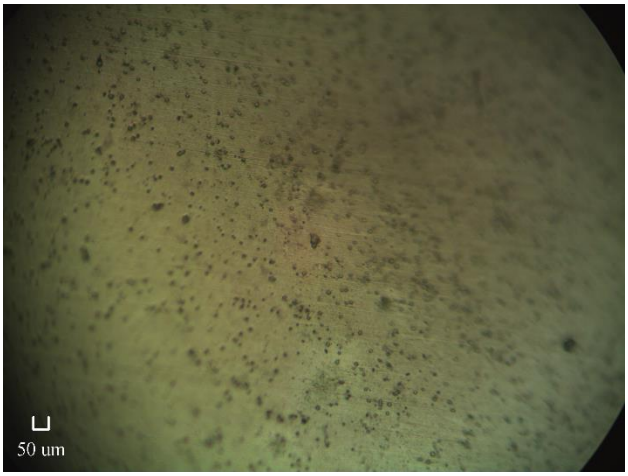

(a)

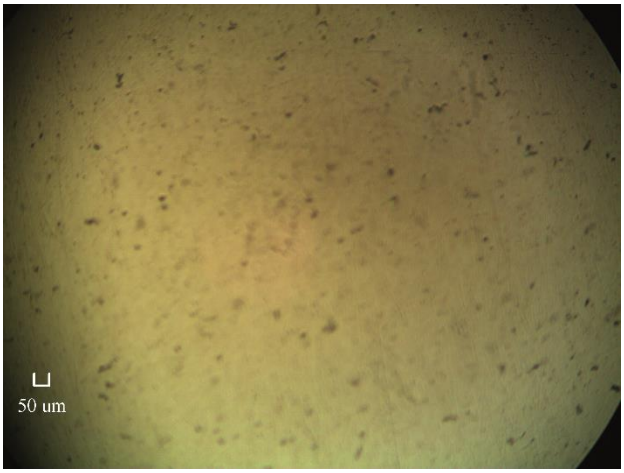

(b)

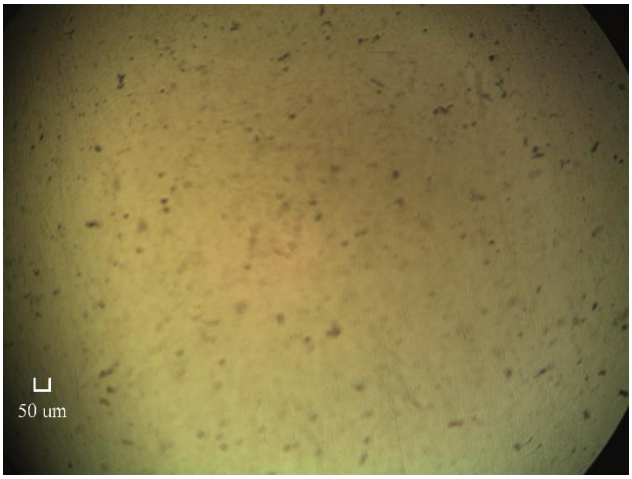

(c)

(d)

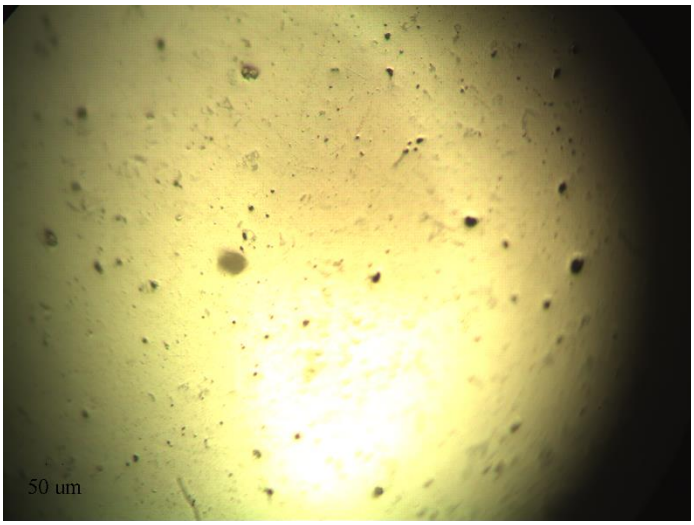

(e)

Fig.38 Polishing of sample at 500X a) 6µm, b) 3µm c) 1µm, d) 0.1µm, e) 0.05µm

3.7.5 Scanning Electron Microscopy:

Scanning Electron Microscopy (SEM) is used to analyze the microstructure and changes at micro level. Two major types of scanning electron microscopes are used: Field Emission and Thermal emission microscopes. JEOL 5910-LV thermal emission with tungsten filament is used for the analysis having magnifying power of 100000X. Conductive materials are used otherwise charging phenomenon may occur that causes blur images than actual. To make the bakelite mounting conductive silver paste is used that touches the metallic specimen to the lower end of the sample.[25]

a) (b)

Fig.39 (a) Sample with silver paste (b) thermal emission scanning electron microscopy

3.7.6 Surface Roughness Testing

Surface Roughness is prime indicator of the machining quality. For checking the surface roughness of machined rods, they are placed on a V-block with grinded upper surfaces. Times Tr-100 portable surface roughness tester is used to check the surface integrity of the machined surface. Each Sample is tested with the repeatability of three times at the angle of 120°. Average Ra values are obtained to analyze the results. Specifications of surface toughness tester is given below:

Sr. No.	Parameter	Value
1	Measuring Range	Ra=0.05-10
2	Stylus Radius	10±2.5μm
3	Stylus angle	90°

Table05 Specifications of surface roughness tester

Fig.40 TR-100 Surface roughness tester

Different unit terminologies are used to measure the surface roughness values as under:

Ra: is arithmetic mean value of the deviation of the profile within sampling length.

$$Ra = \frac{1}{n}\sum_{i=1}^{n}|y_i|$$

Rq: is the root mean square of the deviation of profile within sampling length.

$$Rq = \left(\frac{1}{n}\sum_{i=1}^{n} y_i^2\right)^{\frac{1}{2}}$$

Rz: The sum of two averages five maximum profile peak averages and five maximum profile valley averages within the sampling length.

Ry: The distance between profile peak lines to valley line within sampling length.

3.7.7 Micro hardness Testing:

Fine polished samples are used for calculating the micro hardness under the machined surface at regular interval. Five indents in a row down the machined surface and final indent at the center of the sample as base material hardness test. This experiment is repeated three times and average values are calculated. QAV-1000DAT vicker micro hardness tester is used for this experiment. 25gf load with 10s of dwell time is used. Each indent is marked at the distance of 30 μm form the first to the next according to the ASTM E384 that is distance between indents is atleast three times the mean of diagonals. First indent is marked at the distance of 28.5 μm from the edge. Fig. below shows the schematic of experiment carried out and equipment used with the indent marks.[27]

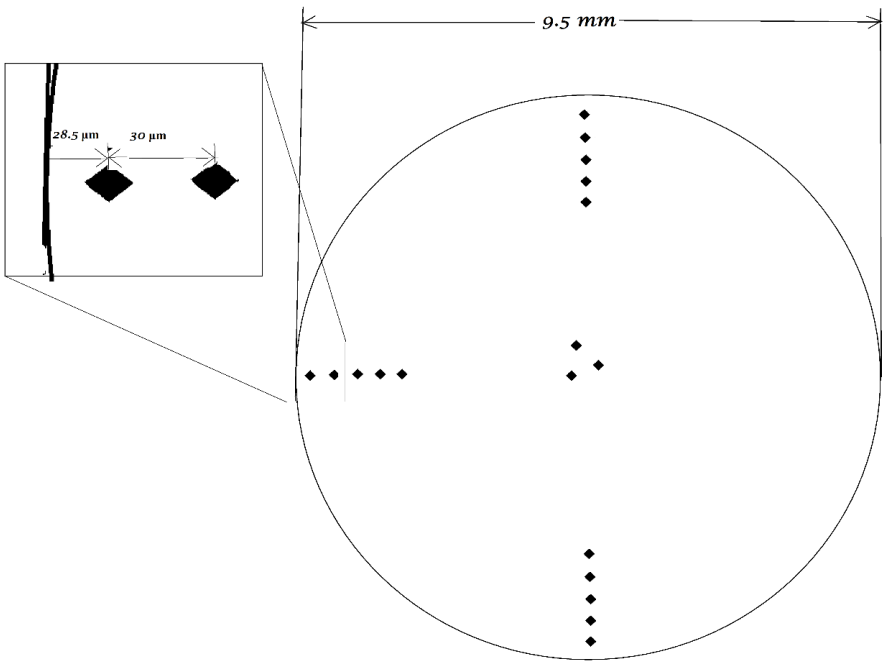

Fig41 Schematic of micro hardness testing

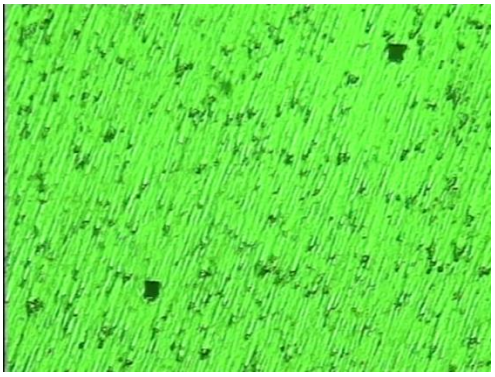

(a)

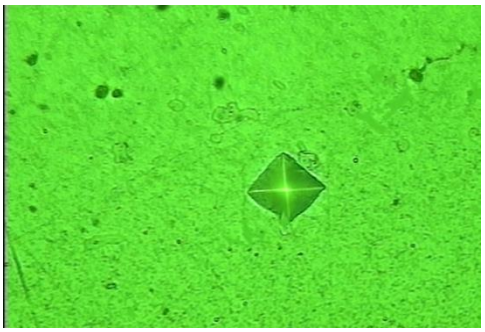

(b)

(c)

Fig42 (a) Two indents shown and their difference (b) Indent (c) QV-1000DAT micro hardness tester

Micro hardness is calculated by measuring the diagonals and calculating the mean of it and using the formula given below:

$$\boldsymbol{Hv = 1.854\ F/d^2}$$

Where; F= Force exerted by the diamond indent

d= mean of diagonal indents[28]

Subsurface damage is calculated by half-life criterion by the formula given below:

$$Hl = (\frac{(max.\ value - min.\ value)}{2}) + min.\ value$$

In this case ,

Max. hardness= 114.8

Base hardness= 109.7

So Hl= 112.2 that lies on 59.49µm

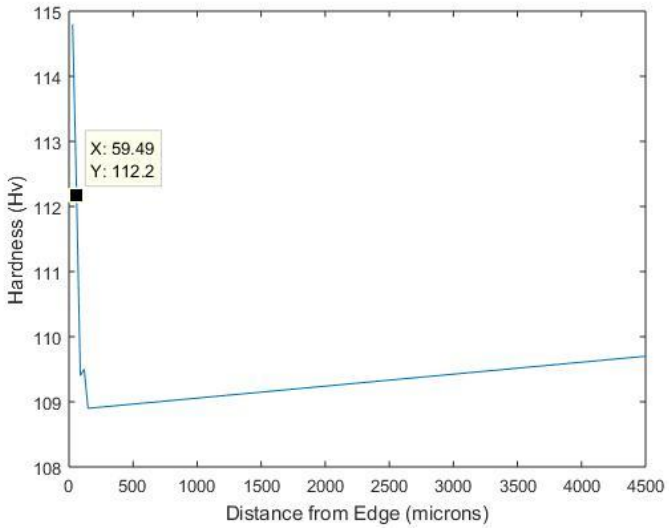

Fig43. Subsurface damage for the machining parameters For feed rate 0.15mm/rev, DOC 1.25mm and Cutting speed 2000 rpm

In the same way all values are calculated by plotting the hardness values at different points of the sample and damage depth is calculated by half-life method according to the obtained hardness value of that sample. Higher values near the machined layer is observed in all samples than the base value.

Chapter 4: Results and Discussions

From the above experiments data was collected that is shown in table below; for all conditions and response parameters values that are surface roughness, fatigue and micro hardness roughness depth.

Sr. no.	Feed rate (mm/rev)	Cutting Speed (rpm)	Depth of cut (mm)	Surface Roughness Ra (μm)	Fatigue Life[1] (cycles)	Subsurface Damage (microns)
1	0.15	1500	1.25	2.553333333	7838	49.66
2	0.15	2000	1.25	2.48	101143	59.49
3	0.15	2000	1.5	4.783333333	148278	73.41
4	0.15	2000	1.75	2.113333333	92930	104.2
5	0.15	2500	1.5	3.44	27982	78.28
6	0.15	2500	1.75	3.626666667	170640	50.2
7	0.2	1500	1.25	3.806666667	53892	52.1
8	0.2	1500	1.5	4.003333333	29384	52.39
9	0.2	2000	1.25	3.896666667	72940	47.69
10	0.2	2000	1.75	3.393333333	50852	114.2
11	0.2	2500	1.5	3.75	61065	76.87
12	0.25	1500	1.5	5.033333333	110240	73.19
13	0.25	2000	1.5	6.28	32508	54.01
14	0.25	2000	1.75	4.883333333	13288	78.27
15	0.25	2500	1.5	5.333333333	35426	55.57
16	0.25	2500	1.75	5.183333333	94971	95
17	0.25	1500	1.25	6.163333333	37402	75.07
18	0.2	2500	1.75	4.093333333	46376	89.8
19	0.2	1500	1.75	5.84	95349	116.3
20	0.15	2500	1.25	3.21	40450	48.8
21	0.2	2500	1.25	5.473333333	33261	79.33
22	0.25	2000	1.25	7.09	41525	62.36
23	0.25	2500	1.25	7.483333333	68785	46.7
24	0.15	1500	1.5	3.41	139168	81.7
25	0.2	2000	1.5	4.82	115360	126.7
26	0.15	1500	1.75	3.973333333	131658	58.03
27	0.25	1500	1.75	8.346666667	59314	63.07

Table Surface roughness, fatigue and subsurface damage measurements for samples

By comparing the two variables to the responses (surface roughness and subsurface damage) we get;

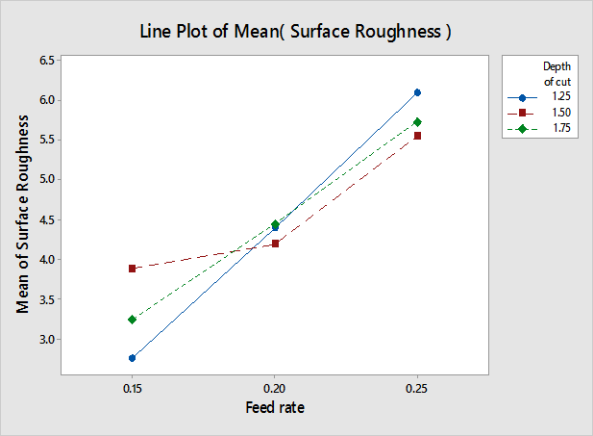

(a)

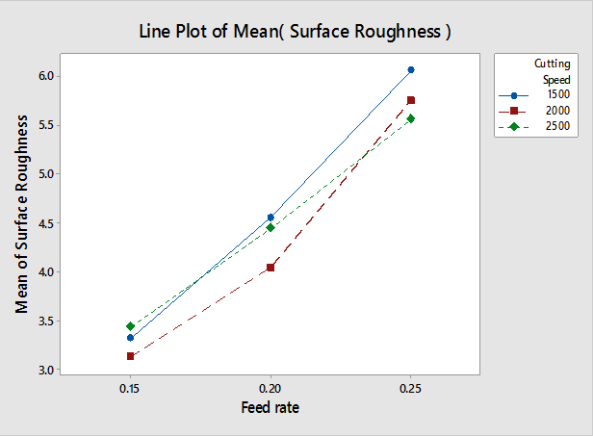

(b)

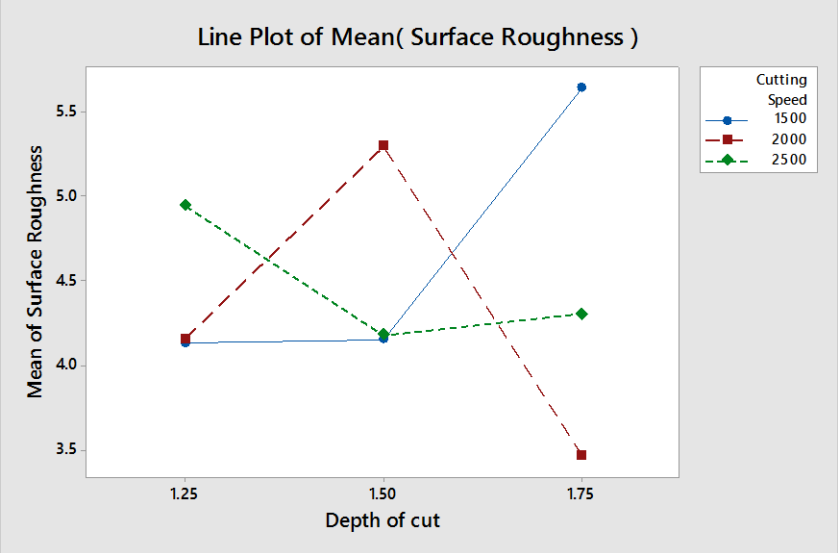

(c)

Fig44 (a) plot of surface roughness against feed rate and depth of cut (b) plot of surface roughness against feed rate and cutting speed (c) plot of surface roughness against depth of cut and cutting speed

In fig44 (a) surface roughness marked behavior with respect to the feed rate and depth of cut, it shows that the feed rate is directly affect the surface roughness value. Increase in feed rate from 0.15 mm/rev to 0.25 mm/rev increases the surface roughness value. Corresponding to the depth of

cut surface roughness increases with increase in depth of cut and correspondently to the feed rate. At feed rate=0.25 mm/rev, depth of cut shows inversely relation to the surface roughness as increase in DOC results in decrease in surface roughness.

In fig44 (b) feed rate and cutting speed is plotted against the surface roughness. Surface roughness increases with increase in feed rate while surface roughness decreases with increase in cutting speed. Cutting speed of 2000rpm is of lowest value.

In fig44 (c) DOC and cutting speed is plotted against the surface roughness. Random behavior is observed as at cutting speed of 1500 rpm incremental trend of surface roughness is observed while for cutting speed 2000 rpm surface roughness is maximum at 1.5mm DOC then decreases.

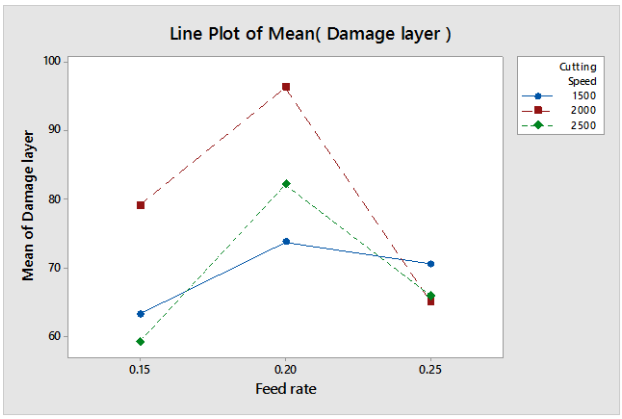

(a)

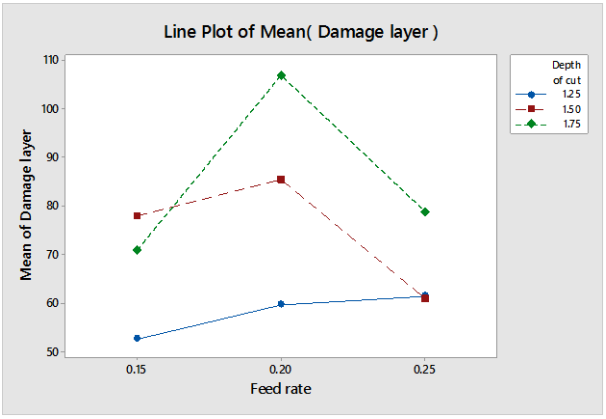

(b)

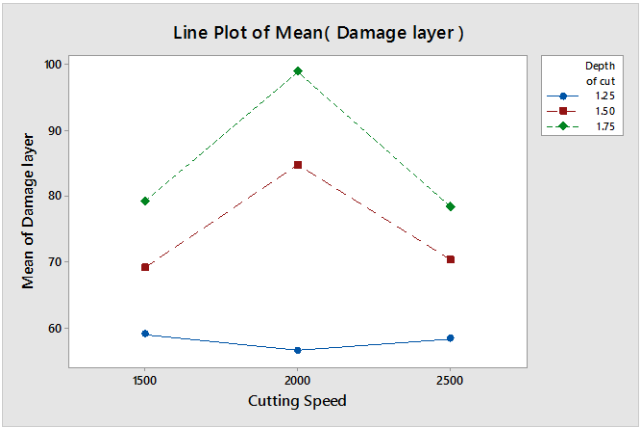

(c)

Fig45 (a) plot of Subsurface damage against feed rate and depth of cut (b) plot of Subsurface damage against feed rate and cutting speed (c) plot of Subsurface damage against depth of cut and cutting speed

In the fig, it is indicated that the maximum values of subsurface damage is at feed rate= 0.2 mm/rev and cutting speed of 2000 rpm. Depth of cut shows relatively the direct relation with the surface roughness as it increases with increase in DOC.

4.1 Optimized Parameters

Surface Roughness is key indicator for the surface quality. It is desirous in some designs but usually it is avoided to increase the value of surface roughness from the specified limit. For that case, machining parameters are selected that get the optimized value for the desired application. Similarly hardening of layer is good in some case but in other side it cause worst effect on the mechanical parameters of the specimen.

For Surface Roughness, minimum value is Ra=2.11 μm at the condition of feed rate= 0.15mm/rev, cutting speed= 2000rpm and depth of cut= 1.75 mm. While maximum surface roughness is Ra=8.34 μm at the condition of feed rate= 0.25 mm/rev, cutting speed= 1500 rpm and depth of cut= 1.75 mm. (ANNEX-A)

For subsurface damage, minimum damage thickness is 46.7 μm at feed rate= 0.25mm/rev, cutting speed= 2500rpm and depth of cut= 1.25 mm and maximum damage thickness is 126.7 μm at feed rate=0.2mm/rev, cutting speed= 2000rpm and depth of cut= 1.5 mm. (ANNEX=B)

For fatigue life, maximum life is 170640 cycles at feed rate= 0.15mm/rev, cutting speed= 2500rpm and depth of cut= 1.75 mm where surface roughness is Ra=3.62 μm and SSD= 50.2μm. While minimum fatigue life is 7838 cycles at feed rate= 0.15mm/rev, cutting speed= 1500rpm and depth of cut= 1.25mm where surface roughness is 2.55μm and SSD= 49.66μm.[1]

4.2 Analysis of Variance

General Linear Model is selected for the analysis and percentage contribution of each parameter.[29]

Subsurface Damage					
Source	DF	SS	MS	**P**	**PC%**
Feed Rate	2	1708.6	854.3	**0**	**12.64618**
Cutting Speed	2	730.5	365.2	**0.00074**	**5.406786**
Depth of Cut	2	3467.2	1733.6	**0**	**25.66243**
FR*CS	4	773	193.2	**0.00148**	**5.721349**
FR*DC	4	1496.3	374.1	**-0.00074**	**11.07484**
DC*CS	4	546.9	136.7	**0.00074**	**4.047873**
FR*CS*DC	8	4788.3	598.5	**0.00222**	**35.44054**
Total	26	13510.8			

Table07 ANOVA and percentage contribution for subsurface damage

Fatigue					
Source	DF	SS	MS	**P**	**%**
Feed Rate	2	8504113943	4252056971	**2.00627E-09**	**17.06156**
Cutting Speed	2	569312525	284656263	**-2.0063E-09**	**1.142195**
Depth of Cut	2	5580358810	2790179405	**0**	**11.19571**
FR*CS	4	5871802814	1467950703	**4.01254E-09**	**11.78043**
FR*DC	4	5430111403	1357527851	**-2.0063E-09**	**10.89428**
DC*CS	4	12291069149	3072767287	**2.00627E-09**	**24.65922**
FR*CS*DC	8	11596933877	1449616735	**-6.0188E-09**	**23.2666**
Total	26	49843702521			

Table08 ANOVA and percentage contribution for Fatigue Life. [1]

Surface Roughness					
Source	DF	SS	MS	**P**	**PC%**
Feed Rate	2	39.124	19.5619	**0.000322**	**62.9413**
Cutting Speed	2	0.6403	0.3202	**-0.00016**	**1.030092**
Depth of Cut	2	0.0946	0.0473	**0**	**0.152189**
FR*CS	4	0.3917	0.0979	**0.000161**	**0.630153**
FR*DC	4	4.7433	1.1858	**0.000161**	**7.630853**
DC*CS	4	14.791	3.6978	**-0.00032**	**23.79524**
FR*CS*DC	8	2.3747	0.2968	**0.000483**	**3.820333**
Total	26	62.1595			
FR*CS*DC	8	11596933877	1449616735	**-6.0188E-09**	**23.2666**
Total	26	49843702521			

Table09 ANOVA and percentage contribution for Surface Roughness

$$PCx = \frac{SSx}{Total\ SS} * 100$$

$$SS_A = \frac{1}{bcn}\sum_{i=1}^{a} y2_{i\ldots} - y2_{\ldots\overline{abcn}}, \qquad SS_B = \frac{1}{acn}\sum_{j=1}^{b} y2_{j\ldots} - y2_{\ldots\overline{abcn}}$$

$$SS_C = \frac{1}{abn}\sum_{k=1}^{c} y2_{k\ldots} - y2_{\ldots\overline{abcn}}$$

$$SS_{AB} = \frac{1}{cn}\sum_{i=1}^{a}\sum_{j=1}^{b} y2_{ij..} - y2_{\ldots\overline{abcn}} \quad -SS_A - SS_B$$

$$SS_{BC} = \frac{1}{an}\sum_{j=1}^{b}\sum_{k=1}^{c} y2_{jk..} - y2_{\ldots\overline{abcn}} \quad -SS_B - SS_C$$

$$SS_{AC} = \frac{1}{bn}\sum_{i=1}^{a}\sum_{k=1}^{c} y2_{ik..} - y2_{\ldots\overline{abcn}} \quad -SS_A - SS_C$$

$$SS_{ABC} = \frac{1}{n}\sum_{i=1}^{a}\sum_{j=1}^{b}\sum_{k=1}^{c} y2_{ijk.} - y2_{\ldots\overline{abcn}} \quad -SS_A - SS_B - SS_C - SS_{AB} - SS_{BC} - SS_{AC}$$

$$SS_{subtotals(ABC)} = \frac{1}{n}\sum_{i=1}^{a}\sum_{j=1}^{b}\sum_{k=1}^{c} y2_{ijk.} - y2_{\ldots\overline{abcn}} \quad ,$$

$$SS_T = \frac{1}{n}\sum_{i=1}^{a}\sum_{j=1}^{b}\sum_{k=1}^{c}\sum_{l=1}^{n} y2_{ijkl} - y2_{\ldots\overline{abcn}} \quad , \qquad SS_E = SS_T - SS_{subtotals(ABC)}$$

Machining parameter	Surface roughness (%)	Fatigue life (%)	Subsurface damage (%)
Feed Rate	**62.94**	**17.06**	12.64
Cutting Speed	1.03	1.14	5.4
Depth of Cut	0.15	11.19	**25.66**
FR*CS	0.63	11.78	5.72
FR*DC	7.63	10.89	11.07
DC*CS	23.79	**24.65**	4.04
FR*CS*DC	3.82	23.26	**35.44**

Table10 Contribution Ratio of response and variables

Table shows that the feed rate is of key importance in determining fatigue life and surface roughness of machined sample. While in subsurface damage depth of cut is most important variable than rest of others.

4.3 Main Effect Plots

Main effect plots of both responses and their variables helped to conclude the relation of each variable with the surface roughness and subsurface damage respectively. These plots are compared with the main effect plots of fatigue life.[1]

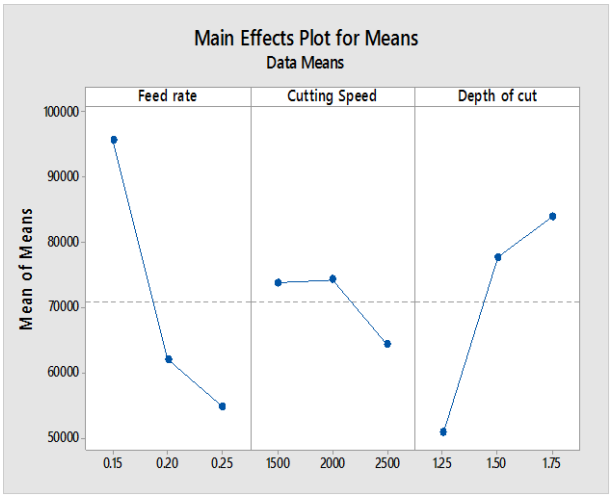

(a)

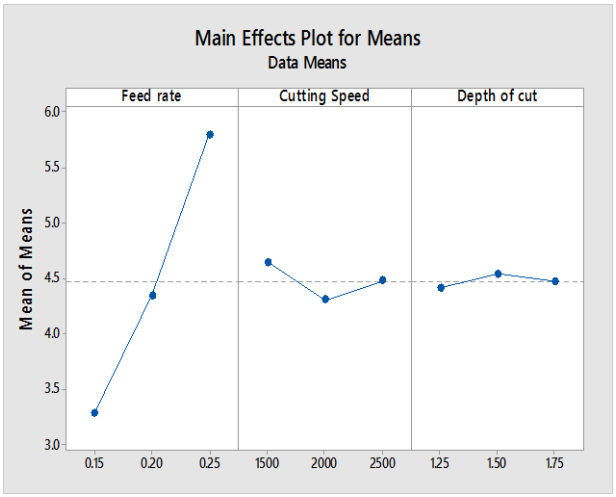

(b)

Fig46 (a) Main effect plot of fatigue life (b) Main effect plot of surface roughness

Fig. shows that the feed rate (most effective parameter for both fatigue life and surface roughness) increases fatigue life increases while in surface roughness increases with increase in feed rate. Same is the case with cutting speed that is inversely proportional to surface roughness. DOC has some contradictive behavior for fatigue life and surface roughness but it has minimum contribution ratio as mentioned in table of contribution ratios. From all parameters, it can be concluded that fatigue life and surface roughness are inversely proportional to each other as fatigue life increases if the surface roughness is minimum for the desired machined surface.

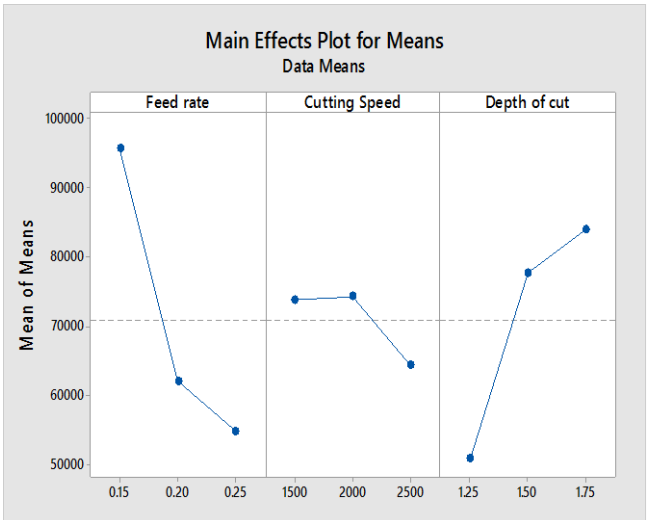

(a)

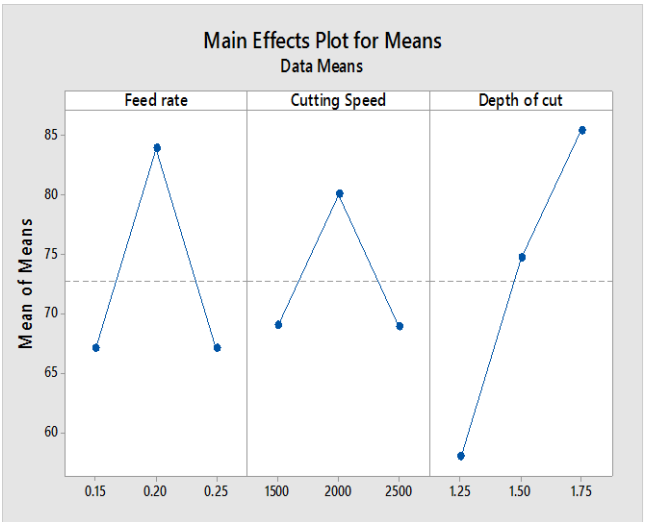

(b)

Fig47 (a) Main effect plot of fatigue life (b) Main effect plot of Subsurface Damage

In fig. feed rate and cutting speed does not show the same trend for fatigue life and subsurface damage. Although depth of cut that is the main contributing machining parameter in subsurface damage has the direct on the fatigue life which means that fatigue life increases as the subsurface damage increases for the variable of depth of cut. No trend shows that the fatigue is not directly depends upon the subsurface damage caused by the machining.

4.4 White Layer Formation

Increase in subsurface hardness near to the machined surface is mainly due to the work hardening, plastic deformation and white layer formation.[6]Due to thermomechanical processes the microstructural changes that formed a layer often appear brighter than the base material that is qhy it is called white layer. It is sometimes desirable but due to safety concerns it is avoided to be formed. Samples are observed to find same phenomenon under scanning electron microscope.[30]

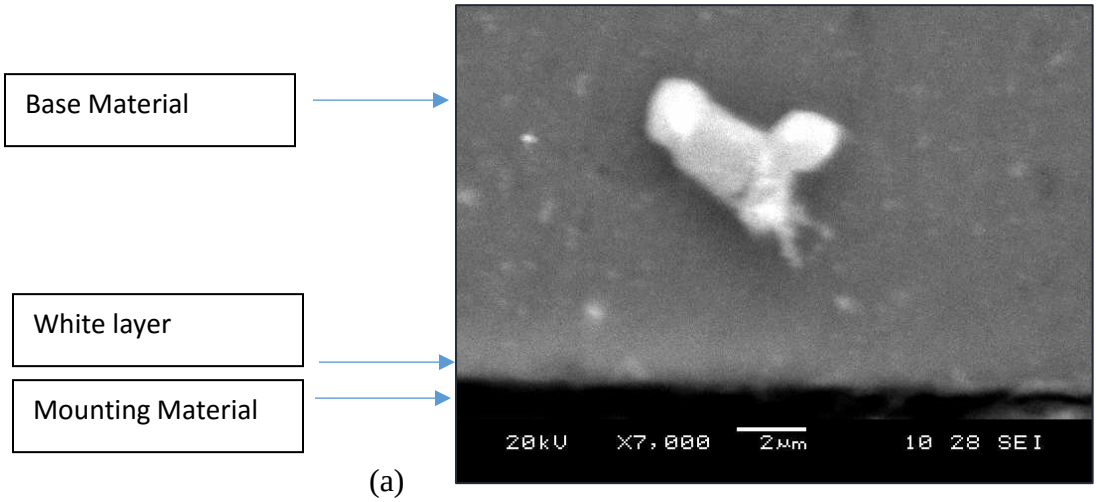

(a)

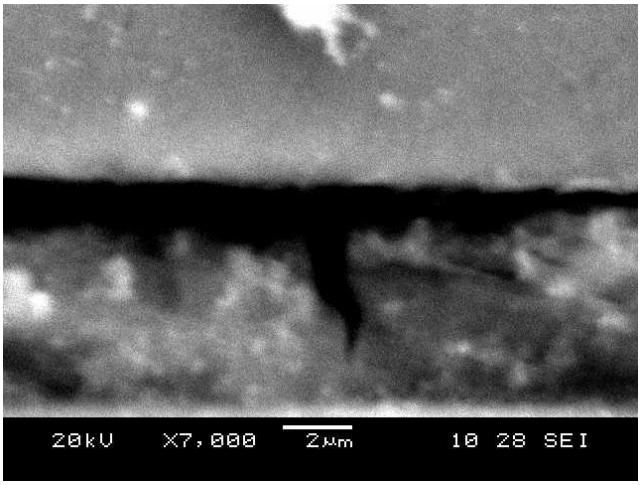

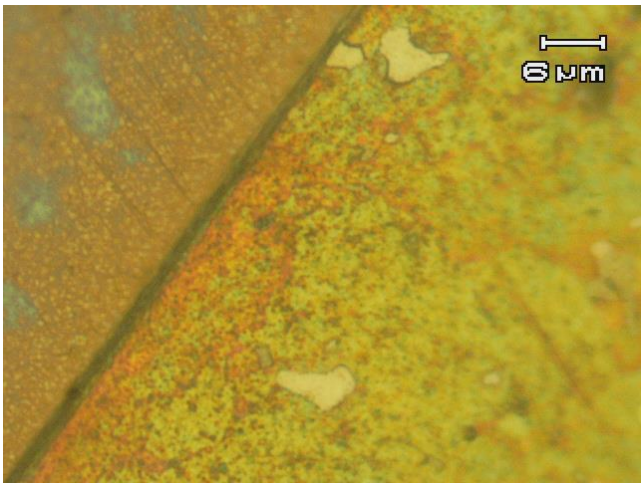

(b) (c)

Fig48 (a) & (b) Scanning electron microscope images for machined samples at 7000X (b) Optical microscope image at 1000X

Fig48 shows that the damage caused by the machining of the material. Thermal changes caused the white layer formation that increases the hardness at upper layer of the machined surface while base material variation is much lower than the upper value.

Chapter 5: Conclusions and Recommendations

5.1 Conclusions

In this research, aluminum 6082-T6 samples are turned at different operating conditions and analyzed for the response parameters like surface roughness and subsurface damage depth and their relation with the fatigue life of the samples. Following conclusions are drawn from the whole experimentations:

- Surface roughness is directly effects the fatigue life of specimen. As increase in surface roughness decreases the fatigue life of the specimen that is mainly due to the crack generates from the upper machined surface.
- From main effect plots, feed rate and cutting speed of surface roughness has inverse trend to the feed rate and cutting speed of fatigue life which means increase in feed rate increases the surface roughness and decreases the fatigue life. Similarly increase in cutting speed decreases the surface roughness value and increases the fatigue life of the specimen. Depth

of cut does not show any prominent role in comparing the surface roughness and fatigue life although it gets least contributing ratio in both response parameters.

- Subsurface damage does not show any direct relation to the fatigue life of the specimen. Main effect plots shows that the depth of cut of subsurface damage and fatigue life has similar trend as increase in depth of cut subsurface damage increases that also results in increase in fatigue life.
- Due to thermo-mechanical effect of the machining the upper surface of the specimen get hardened due to white layer formation. Similar trend is observed in all samples that 15-20% increase in hardness at lower than the base material of about (110Hv).
- For subsurface damage, depth of cut is the most contributing machining parameter. Maximum subsurface damage is observed at feed rate of 0.2mm/rev and cutting speed of 2000 rpm.
- Least subsurface damage of 46.7μm is caused at the condition of feed rate=0.25mm/rev, cutting speed= 2500 rpm and depth of cut of 1.25mm. While maximum damaged layer thickness of 126.7 μm is observed at feed rate= 0.2 mm/rev, cutting speed=2000rpm and depth of cut=1.5 mm.

- For surface roughness most dominating machining parameter is feed rate that contribute up to 62.9% of total effect. Feed rate shows direct trend that surface roughness increase with increase in feed rate and vice versa. For cutting speed this trend is opposite that cutting speed increases and surface roughness decreases.
- For Surface Roughness, minimum value is Ra=2.11 μm at the condition of feed rate= 0.15mm/rev, cutting speed= 2000rpm and depth of cut= 1.75 mm. While maximum surface roughness is Ra=8.34 μm at the condition of feed rate= 0.25 mm/rev, cutting speed= 1500 rpm and depth of cut= 1.75 mm.

5.2 Recommendations for future work

For the future work, following dimensions is recommended related to this work:

- Residual stresses generated by turning at different machining parameters by X-RD.
- Force induced by tool at different parameters.
- Change in natural frequency and damping coefficient due to change in outer hardened layer.

ANNEXURE-A: Detailed result of surface roughness experiment.

Sr. no.	Feed rate (mm/rev)	Cutting Speed (rpm)	Depth of cut (mm)	Surface Roughness (Ra) 1 (µm)	Surface Roughness (Ra) 2 (µm)	Surface Roughness (Ra) 3 (µm)	Surface Roughness avg. Ra (µm)
1	0.15	1500	1.25	2.4	2.74	2.52	2.553333333
2	0.15	2000	1.25	2.6	2.5	2.34	2.48
3	0.15	2000	1.5	5.03	4.6	4.72	4.783333333
4	0.15	2000	1.75	2.1	2.13	2.11	2.113333333
5	0.15	2500	1.5	3.43	3.57	3.32	3.44
6	0.15	2500	1.75	3.92	3.15	3.81	3.626666667
7	0.2	1500	1.25	3.84	3.68	3.9	3.806666667
8	0.2	1500	1.5	4.06	4.09	3.86	4.003333333
9	0.2	2000	1.25	3.81	3.78	4.1	3.896666667
10	0.2	2000	1.75	3.43	3.42	3.33	3.393333333
11	0.2	2500	1.5	3.76	3.69	3.8	3.75
12	0.25	1500	1.5	5.61	4.93	4.56	5.033333333
13	0.25	2000	1.5	6.3	6.15	6.39	6.28
14	0.25	2000	1.75	4.82	4.91	4.92	4.883333333
15	0.25	2500	1.5	5.34	5.26	5.4	5.333333333
16	0.25	2500	1.75	5.18	5.11	5.26	5.183333333
17	0.25	1500	1.25	6.53	6.07	5.89	6.163333333
18	0.2	2500	1.75	4.04	4.18	4.06	4.093333333
19	0.2	1500	1.75	5.9	5.93	5.69	5.84
20	0.15	2500	1.25	2.87	3.43	3.33	3.21
21	0.2	2500	1.25	5.66	5.49	5.27	5.473333333
22	0.25	2000	1.25	6.92	7.17	7.18	7.09
23	0.25	2500	1.25	8.13	7.2	7.12	7.483333333
24	0.15	1500	1.5	3.22	3.45	3.56	3.41
25	0.2	2000	1.5	4.66	4.92	4.88	4.82
26	0.15	1500	1.75	3.83	4.21	3.88	3.973333333
27	0.25	1500	1.75	8.48	7.9	8.66	8.346666667

ANNEXURE-B: Detailed results of micro hardness test

Sample no. 1			Sample no. 2		
	Hv	**Hv (avg.)**		**Hv**	**Hv (avg.)**
Indent 1	119	118.367	**Indent 1**	120	114.8
	118.6			109	
	117.5			115.4	
Indent 2	114.1	113.733	**Indent 2**	117	112.267
	112.8			108.6	
	114.3			111.2	
Indent 3	113.1	113.133	**Indent 3**	111.3	109.4
	113.7			109	
	112.6			107.9	
Indent 4	112.1	111.967	**Indent 4**	116	109.533
	112			107	
	111.8			105.6	
Indent 5	112.3	112.067	**Indent 5**	113.1	108.933
	112.1			107	
	111.8			106.7	
Indent 6 (center)	111.4	111.9	**Indent 6 (center)**	105.6	109.7
	112.4			109.5	
				114	
Sample no. 3			Sample no. 4		
	Hv	**Hv (avg.)**		**Hv**	**Hv (avg.)**
Indent 1	101.8	103.1	**Indent 1**	101	103.733
	104.3			108.8	
	103.2			101.4	
Indent 2	99.8	101.633	**Indent 2**	101.8	102.667
	103			105	
	102.1			101.2	
Indent 3	97.2	98.6667	**Indent 3**	101.2	103.067
	99.5			107	
	99.3			101	
Indent 4	94.3	97.8	**Indent 4**	104.3	101.833
	101.8			101	
	97.3			100.2	
Indent 5	95	95.7333	**Indent 5**	103.5	101.633
	94.8			101.2	
	97.4			100.2	
Indent 6 (center)	97	97.45	**Indent 6 (center)**	100.2	101.167
	97.9			101.5	
				101.8	

Sample no. 5			Sample no. 6		
	Hv	**Hv (avg)**		**Hv**	**Hv (avg)**
Indent 1	110.4	112.733	**Indent 1**	120	116.967
	115			114.1	
	112.8			116.8	
Indent 2	111.3	113.233	**Indent 2**	116	113.333
	120			111	
	108.4			113	
Indent 3	114.1	111.033	**Indent 3**	107.7	112
	108			116	
	111			112.3	
Indent 4	113.1	110.567	**Indent 4**	114.1	112.067
	108.6			112	
	110			110.1	
Indent 5	111	110.233	**Indent 5**	109.5	108.667
	110.2			109.2	
	109.5			107.3	
Indent 6 (center)	113	110.933	**Indent 6 (center)**	111	111.733
	110.6			112	
	109.2			112.2	
Sample no. 7			Sample no. 8		
	Hv	**Hv (avg)**		**Hv**	**Hv (avg)**
Indent 1	125.5	125.767	**Indent 1**	158.8	161.667
	128.2			160.1	
	123.6			166.1	
Indent 2	124.3	124.167	**Indent 2**	151.5	150.533
	123.4			147.7	
	124.8			152.4	
Indent 3	123.1	123.3	**Indent 3**	141.4	144.9
	123.6			146.5	
	123.2			146.8	
Indent 4	123.5	123.267	**Indent 4**	138.8	141.767
	123.2			146	
	123.1			140.5	
Indent 5	123.8	123.067	**Indent 5**	138.2	142.6
	123.2			144.6	
	122.2			145	
Indent 6 (center)	122.2	123.233	**Indent 6 (center)**	138.2	140.067
	123.9			140.2	
	123.6			141.8	

Sample no. 9			Sample no. 10		
	Hv	**Hv (avg)**		**Hv**	**Hv (avg)**
Indent 1	125.3	124	**Indent 1**	117	113.467
	122.6			110.4	
	124.1			113	
Indent 2	115	115.6	**Indent 2**	118	115.1
	116			114.1	
	115.8			113.2	
Indent 3	120	110.367	**Indent 3**	126.4	116.633
	101			110.4	
	110.1			113.1	
Indent 4	113.1	110.433	**Indent 4**	117	112.767
	109.5			109	
	108.7			112.3	
Indent 5	112.2	111.3	**Indent 5**	116	111.333
	111.3			107	
	110.4			111	
Indent 6 (center)	113.1	113.233	**Indent 6 (center)**	110	110.167
	113.1			111.5	
	113.5			109	
Sample no. 11			Sample no. 12		
	Hv	**Hv (avg)**		**Hv**	**Hv (avg)**
Indent 1	113.1	112.633	**Indent 1**	105	104.967
	112.2			105.1	
	112.6			104.8	
Indent 2	112.3	111.767	**Indent 2**	104.3	103.867
	111.3			104	
	111.7			103.3	
Indent 3	108.6	108.3	**Indent 3**	99.2	100.733
	109			102	
	107.3			101	
Indent 4	109.5	107.7	**Indent 4**	101.8	101.333
	107.1			103	
	106.5			99.2	
Indent 5	108.6	107.4	**Indent 5**	102.7	100.7
	107.8			99.9	
	105.8			99.5	
Indent 6 (center)	105	106.767	**Indent 6 (center)**	103	99.6333
	101.3			99	
	114			96.9	

Sample no. 13			Sample no. 14		
	Hv	**Hv (avg)**		**Hv**	**Hv (avg)**
Indent 1	114.1	116.467	**Indent 1**	102.6	108.7
	119			115	
	116.3			108.5	
Indent 2	112.2	112.067	**Indent 2**	101.8	107.467
	112.2			113.1	
	111.8			107.5	
Indent 3	108.1	109.367	**Indent 3**	99.2	106.033
	110.5			112.9	
	109.5			106	
Indent 4	106.8	108.2	**Indent 4**	98.9	103.833
	109.5			108.5	
	108.3			104.1	
Indent 5	106	107.8	**Indent 5**	98.5	103.033
	109.3			106.8	
	108.1			103.8	
Indent 6 (center)	109.5	108.5	**Indent 6 (center)**	104.8	104.267
	108.2			104.5	
	107.8			103.5	
Sample no. 15			Sample no. 16		
	Hv	**Hv (avg)**		**Hv**	**Hv (avg)**
Indent 1	119	118.9	**Indent 1**	110.4	109.8
	119			110.4	
	118.7			108.6	
Indent 2	126.4	116.367	**Indent 2**	110.4	111.2
	106			116	
	116.7			107.2	
Indent 3	119	114.267	**Indent 3**	109.5	107.867
	109.5			106.8	
	114.3			107.3	
Indent 4	116	115.9	**Indent 4**	117	106.9
	116			102.6	
	115.7			101.1	
Indent 5	115	114.767	**Indent 5**	121	108.4
	115			101.8	
	114.3			102.4	
Indent 6 (center)	115	114.367	**Indent 6 (center)**	101.8	104.3
	114.2			105.1	
	113.9			106	

Sample no. 17 (55)			Sample no. 18 (57)		
	Hv	**Hv (avg)**		**Hv**	**Hv (avg)**
Indent 1	160.2	160.233	**Indent 1**	104.3	104.2
	159.2			104	
	161.3			104.3	
Indent 2	159.4	159.433	**Indent 2**	103.5	103.867
	158.8			104.3	
	160.1			103.8	
Indent 3	144.8	145.033	**Indent 3**	101.8	101.9
	145.2			101.8	
	145.1			102.1	
Indent 4	142.2	142.6	**Indent 4**	100.3	99.8
	143.1			99.3	
	142.5			99.8	
Indent 5	142.9	142.4	**Indent 5**	97.9	98.8
	144.2			100.3	
	140.1			98.2	
Indent 6 (center)	142.6	142.6	**Indent 6 (center)**	99.5	99.4667
	143			101.8	
	142.2			97.1	
Sample no. 19 (58)			Sample no. 20 (59)		
	Hv	**Hv (avg)**		**Hv**	**Hv (avg)**
Indent 1	158.8	160.933	**Indent 1**	134	131.333
	156.4			129	
	167.6			131	
Indent 2	156.7	155.933	**Indent 2**	135	133.333
	156.2			132	
	154.9			133	
Indent 3	155.5	157.4	**Indent 3**	122	127.033
	161.8			129	
	154.9			130.1	
Indent 4	154.3	154.5	**Indent 4**	124	124.5
	156.9			125.6	
	152.3			123.9	
Indent 5	153.9	153.133	**Indent 5**	122	120.2
	155.4			121.3	
	150.1			117.3	
Indent 6 (center)	148.2	148.5	**Indent 6 (center)**	116	114.333
	148.8			112	
	145.7			115	

Sample no. 21 (60)			Sample no. 22 (61)		
	Hv	**Hv (avg)**		**Hv**	**Hv (avg)**
Indent 1	128	128.167	**Indent 1**	167.9	167.8
	130.1			162.9	
	126.4			172.6	
Indent 2	128.6	124.2	**Indent 2**	155.4	160.567
	120			158.4	
	124			167.9	
Indent 3	120	114.9	**Indent 3**	154.6	156.5
	109.5			159.1	
	115.2			155.8	
Indent 4	116	109.233	**Indent 4**	152.3	153.4
	100.7			154.4	
	111			153.5	
Indent 5	108	107.767	**Indent 5**	151.2	150.8
	108			151.1	
	107.3			150.1	
Indent 6 (center)	108	107.1	**Indent 6 (center)**	152	152.267
	106.4			154.7	
	106.9			150.1	
Sample no. 23 (62)			Sample no. 24 (71)		
	Hv	**Hv (avg)**		**Hv**	**Hv (avg)**
Indent 1	133.3	128.033	**Indent 1**	160.8	157.833
	122.1			155.7	
	128.7			157	
Indent 2	118	117.267	**Indent 2**	159.5	154.5
	116			149.8	
	117.8			154.2	
Indent 3	116	114.233	**Indent 3**	144.8	147.6
	112.2			150.4	
	114.5			147.6	
Indent 4	114.6	115.367	**Indent 4**	143.5	140.533
	117			138.3	
	114.5			139.8	
Indent 5	114.1	115	**Indent 5**	139.2	140.1
	116			142.2	
	114.9			138.9	
Indent 6 (center)	115	115.033	**Indent 6 (center)**	137	140.733
	113.1			146	
	117			139.2	

Sample no. 25 (72)			Sample no. 26 (73)		
	Hv	**Hv (avg)**		**Hv**	**Hv (avg)**
Indent 1	153.3	141.667	**Indent 1**	144.8	142.467
	128			140.8	
	143.7			141.8	
Indent 2	138.3	138.133	**Indent 2**	138.3	138.167
	138.9			138.3	
	137.2			137.9	
Indent 3	133.3	133.2	**Indent 3**	143.5	138.5
	132.2			135.7	
	134.1			136.3	
Indent 4	126.4	127.867	**Indent 4**	138.3	136.167
	132.1			134.5	
	125.1			135.7	
Indent 5	117	116.5	**Indent 5**	145	135.4
	116.2			131	
	116.3			130.2	
Indent 6 (center)	106.8	108	**Indent 6 (center)**	139	134
	106.8			132.1	
	110.4			130.9	

Sample no. 27 (74)		
	Hv	**Hv (avg)**
Indent 1	156.7	150.067
	146.2	
	147.3	
Indent 2	154.4	146.8
	139.5	
	146.5	
Indent 3	153.5	141.733
	130.5	
	141.2	
Indent 4	153.5	142.1
	138.3	
	134.5	
Indent 5	153.5	141.033
	130	
	139.6	
Indent 6 (center)	149.2	142
	139.6	
	137.2	

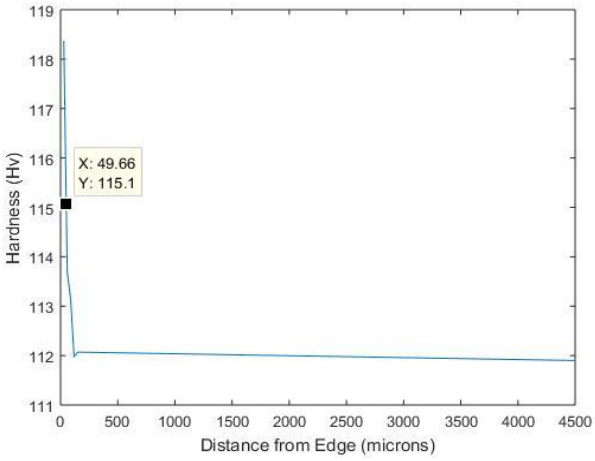

(sample 1)

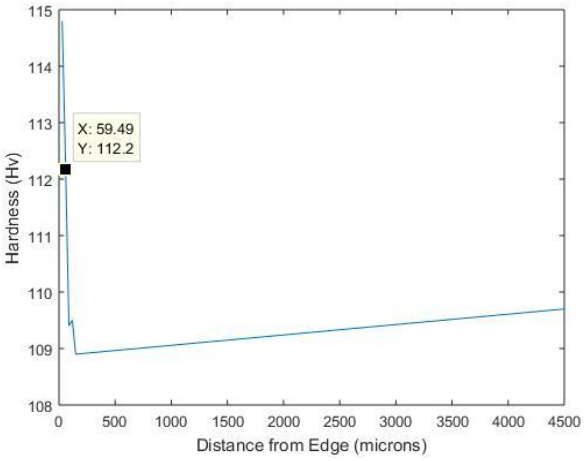

(sample 2)

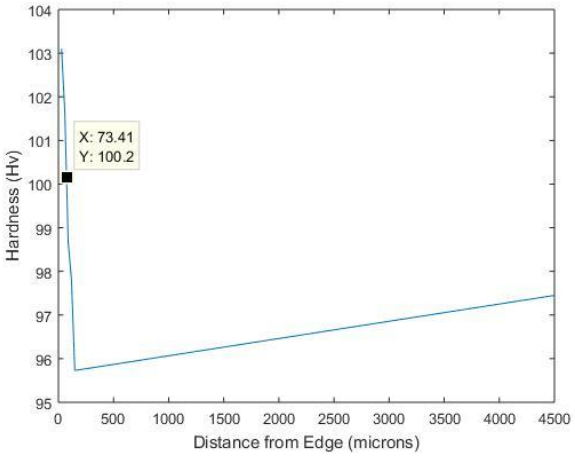

(Sample 3)

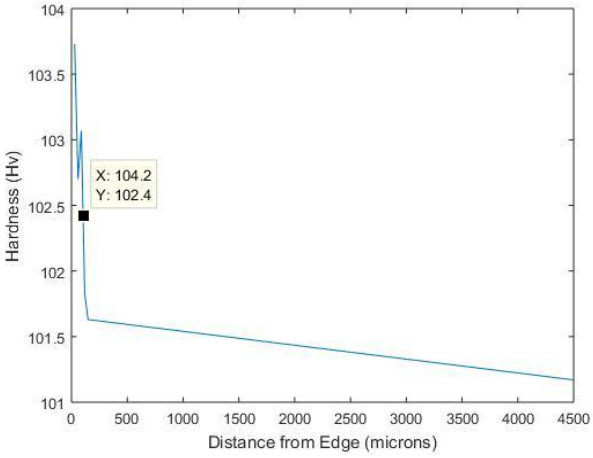

(Sample 4)

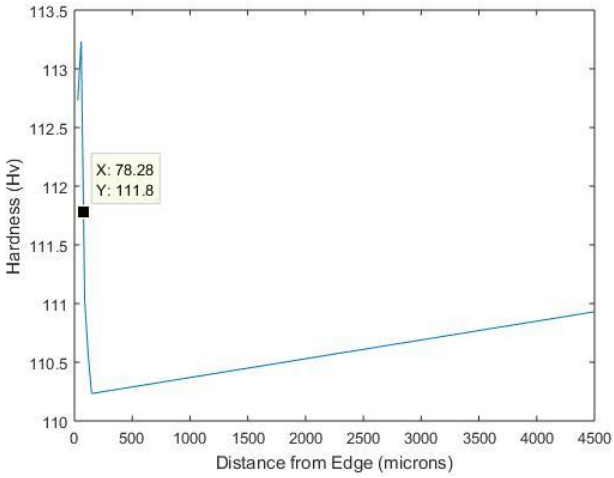

(Sample 5)

References:

[1] Jamshaid, M., *Effect of Machining on Fatigue life of Aerospace Grade Aluminum Alloy (Al 6082-T6).* Masters Thesis, National University of Sciences and Technology, Islamabad, 2012.

[2]. Mufti, R.A., *Mechanical and Microstructure Investigation of Weld based rapid Prototyping* Phd Thesis: p. 258.

[3]. **A.Silli, S.M.a., *Mechanical Behaviour of 6082-T6 aluminum alloy weld.* Dipartimento Chimica Industriale e Ingegneria dei Materiali - Università di Messina - Italy.

[4]. BLAINEAUa, R.L., P. DARNISa, N. DARBOISb, O. CAHUCa, J. NEAUPORT, *Relations between subsurface damage depth and surface roughness using the Abbott Firestone curve.* 21ème Congrès Français de Mécanique, 2013.

[5]. DOBRESCU, T.i.G.a.P., N[icoleta] - E[lisabeta]; and C.o.B. OPRAN, A[nca] M[onica], *SUBSURFACE DAMAGE IN GRINDING SILICON CERAMICS.* Proceedings of the 23rd International DAAAM Symposium, 2012. **23**: p. 102-106.

[6]. Durul Ulutan, T., *Machining induced surface integrity in titanium and nickelalloys: A review.* InternationalJournalofMachineTools&Manufacture, 2011. **51**: p. 250-280.

[7]. F. Pusaveca, H. Hamdib, J. Kopaca, I.S. Jawahirc, *Surface integrity in cryogenic machining of nickel based alloy—Inconel 718.* Journal of Materials Processing Technology, 2011. **211**: p. 773-783.

[8]. Harrison, I.S., *DETECTING WHITE LAYER IN HARD TURNED COMPONENTS USING NON-DESTRUCTIVE METHODS.* 2004. **Georgia Institute of Technology**.

[9]. Hassanpour, H., et al., *Investigation of surface roughness, microhardness and white layer thickness in hard milling of AISI 4340 using minimum quantity lubrication.* Journal of Cleaner Production, 2016. **120**: p. 124-134.

[10]. Iman HEJAZI, S.E.M., *Mechanical and metallurgical characterization of AA6061 friction stir welded joints using microhardness map.* Trans. Nonferrous Met. Soc. China, 2016. **26**: p. 2313−2319.

[11]. Long Wan, Y.H., Zongliang Lv, Shixiong Lv, Jicai Feng, *Effect of self-support friction stir welding on microstructure and microhardness of 6082-T6 aluminum alloy joint.* Materials and Design, 2014. **55**(2014): p. 197–203.

[12]. Sandeep Rathee1*, S.M., Arshad Noor Siddiquee2, Manu Srivastava1, and S.K. Sharma, *Process parameters optimization for enhanced microhardness of AA 6061/ SiC surface composites fabricated via Friction Stir Processing (FSP).* Materials Today: Proceedings, 2016. **3**(2016): p. 4151-4156.

[13]. J. Sun, Y.B.G., *A comprehensive experimental study on surface integrity by end milling Ti–6Al–4V.* Journal of Materials Processing Technology, 2009. **209**: p. 4036–4042.

[14]. Jian Wang, Y.L., Jinghua Han,Qiao Xu,Yinbiao Guo, *Evaluating subsurface damage in optical glasses.* Journal of the European Optical Society, 2011. **6**: p. 11001.

[15]. L. C. LEE*, L.C.L., V. NARAYANAN* and V. C. VENKATESH*, *QUANTIFICATION OF SURFACE DAMAGE OF TOOL STEELS AFTER EDM.* International Journal of Machine Tools & Manufacture, 1988. **28**: p. 359-372.

[16]. M-B. Mhamdia, b., *, M. Boujelbenea,c, E. Bayraktara, A. Zghalb, *Surface Integrity of Titanium Alloy Ti-6Al-4V in Ball end Milling.* Physics Procedia, 2012. **25**: p. 355 – 362.

[17]. McCurry, N.M., *Aluminum temperature coefficient of resistance vs. grain structure.* Theses and Dissertations, 1993: p. 155.

[18]. Jinming Zhou, a., Volodymr Bushlya,b, Ru Lin Peng,c and Jan-Eric Stahl,d, *Identification of Subsurface Deformation in Machining of Inconel 718.* Applied Mechanics and Materials, 2012. **117-119**: p. 1681-1688.

[19]. LI Sheng-yi(李圣怡), W.Z.王.卓., WU Yu-lie(吴宇列), *Relationship between subsurface damage and surface roughness of ground optical materials.* J. Cent. South Univ. Technol., 2007: p. 04−0546−06.

[20] Meenu Gupta, S.K., *Investigation of surface roughness and MRR for turning of UD-GFRP using PCA and Taguchi method.* Engineering Science and Technology, an International Journal, 2015. **18**(2015): p. 70-81.

[21]. M. Tiryakioğlu a, n., J.S.Robinson b, M.A.Salazar-Guapuriche c, Y.Y.Zhao d, P.D.Eason a, *Hardness–strengthrelationshipsinthealuminumalloy7010.* Materials Science & Engineering, 2015. **631**: p. 196-200.

[22]. Ohta, T., *Prediction of subsurface damage depth of ground brittle materials by surface profiling.* international Journal of Machine Tools & Manufacturing, 2007. **2**: p. 109-124.

[23]. Omar Fergania, Y.S., Steven Y. Lianga, *Effect of Temperature on the Subsurface Microstructure and Mechanical Properties of AA 7075-T6 in Machining.* 2nd CIRP 2nd CIRP Conference on Surface Integrity (CSI), 2014. **13**: p. 181-185.

[24]. Saleh N. Alhajeri a, Khaled J. Al-Fadhalahb, Abdulla I. Almazrouee a, Terence G. Langdon, *Microstructure andmicrohardness of an Al-6061metal matrix composite processed by high-pressure torsion.* Materials Characterization, 2016. **118**(2016): p. 270–278.

[25]. E. Cerri, E.E., *Metallography of Aluminium alloys.* Dipartimento di Meccanica, Università di Ancona-Italy.

[26]. Zipperian, D.C., *Metallographic Specimen Preparation Basics.* Pace Technologies.

[27]. Xinkai Ma, F.L., Jun Cao, Jinghui Li, Han Chen, Chen Zhao, *Vickersmicrohardness andmicrostructure relationship of Ti-6Al-4V alloy under cyclic forward-reverse torsion and monotonic torsion loading.* Materials and Design, 2017. **114**(2017): p. 271–281.

[28]. ZHANG, J.M., Z.J. PEI, and J.G. SUN, *Subsurface Damage Measurement in Silicon Wafers by Laser Scattering.* NAMRC XXX, 2002.

[29]. Ross, P.J., *Taguchi Technique for quality engineering.* 5.14, 2nd Edition.

[30]. Yusuf Kaynaka, T.L.I.S.J., *Cryogenic Machining-Induced Surface Integrity: A Review and Comparison with Dry, MQL, and Flood-Cooled Machining.* Machining Science and Technology:, 2014. **18:2**(149-198).